REVISED MANUSCRIPT

A strong CO_2 sink enhanced by eutrophication in a tropical coastal embayment (Guanabara Bay, Rio de Janeiro, Brazil)

Luiz C. Cotovicz Jr.[1,2,*], Bastiaan A. Knoppers[1], Nilva Brandini[1], Suzan J. Costa Santos[1], and Gwenaël Abril[1,2]

[1] Programa de Geoquímica, Universidade Federal Fluminense, Outeiro São João Batista s/n, 24020015, Niterói, RJ, Brazil.

[2] Laboratoire Environnements et Paléoenvironnements Océaniques et Continentaux (EPOC), CNRS, Université de Bordeaux, Allée Geoffroy Saint-Hilaire, 33615 Pessac Cedex France.

[*] Correspondance to Luiz C. Cotovicz Jr (lccjunior@id.uff.br)

Abstract

In contrast to its small surface area, the coastal zone plays a disproportionate role in the global carbon cycle. Carbon production, transformation, emission and burial rates at the land-ocean interface are significant at the global scale, but still poorly known, especially in tropical regions. Surface water pCO_2 and ancillary parameters were monitored during nine field campaigns between April 2013 and April 2014 in Guanabara Bay, a tropical eutrophic to hypertrophic semi-enclosed estuarine embayment surrounded by the city of Rio de Janeiro, SE-Brazil. Water pCO_2 varied between 22 and 3715 ppmv in the Bay showing spatial, diurnal and seasonal trends that mirrored those of dissolved oxygen (DO) and Chlorophyll *a* (Chl *a*). Marked pCO_2 undersaturation was prevalent in the shallow, confined and thermally stratified waters of the upper bay, whereas pCO_2 oversaturation was restricted to sites close to the small river mouths and small sewage channels, which covered only 10 % of the bay´s area. Substantial daily variations in pCO_2 (up to 395 ppmv between dawn and dusk) were also registered and could be integrated temporally and

spatially for the establishment of net diurnal, seasonal and annual CO_2 fluxes. In contrast to other estuaries worldwide, Guanabara Bay behaved as a net sink of atmospheric CO_2, a property enhanced by the concomitant effects of strong radiation intensity, thermal stratification, and high availability of nutrients, which promotes phytoplankton development and net autotrophy. The calculated CO_2 fluxes for Guanabara Bay ranged between -9.6 to -18.3 mol C m^{-2} yr^{-1}, in the same order of magnitude of the organic carbon burial and organic carbon inputs from the watershed. The positive and high net community production (52.1 mol C m^{-2} yr^{-1}) confirms the high carbon production in the bay, and its autotrophic status apparently enhanced by eutrophication. Our results show that global CO_2 budgetary assertions still lack information on tropical, marine-dominated estuarine systems, which are affected by thermal stratification and eutrophication and behave specifically with respect to atmospheric CO_2.

Key words: CO_2 fluxes, eutrophication, estuarine embayment, tropical, SE-Brazil.

1 Introduction

The rising of atmospheric CO_2 concentration in the last decades has worldwide concern, mainly due to global atmospheric temperature increases (Allen et al., 2009; Matthews et al., 2009) and ocean acidification (Doney et al., 2009). The oceans are known to act as the major sink of atmospheric CO_2, with well quantified air–sea exchange and uptake of excess anthropogenic CO_2 (Takahashi et al., 2002; Sabine et al., 2004; Orr et al., 2005). The coastal ocean, however, is still subject to controversy and poorly understood due to its intrinsic intra- and inter-specific heterogeneity. The lack of sufficient studies covering the spatial and temporal variability with a common standardized sampling strategy and methodology and the manifold diverse types of ecosystems types (estuaries, deltas, embayments and coastal lagoons) affected by multiple external and internal sources, are some of the reasons for these uncertainties (Gattuso et al., 1998; Borges, 2005; Chen et al., 2013; Cloern et al., 2014). Despite the small surface area of the coastal ocean of about 7 % of the global ocean, it exerts a disproportionately large influence upon the carbon cycle, especially on the role of primary production, remineralisation and sedimentation of organic matter (Gattuso et al., 1998; Wollast, 1998). Coastal ecosystems receive material from land via river inputs, submerged groundwater discharge, atmospheric deposition, as well as from the adjacent open ocean. The climatological regime has great influence over these areas, and contributes to the great variability of biogeochemical

processes in space and time. In addition, approximately 37% of human population lives within 100 km of coastline (Cohen et al., 2007), making this area subject to intense human impact upon the marine environment, including enhanced loading of nutrients, suspended matter, organic and inorganic matter with associated pollutants, and also overfishing (Bauer et al., 2013).

Several authors have demonstrated that the CO_2 emissions from estuaries are globally significant (Borges and Abril, 2011; Chen et al., 2013). Total ecosystem respiration generally exceeds gross primary production in most estuaries (Gattuso et al., 1998), which are net heterotrophic and sources of atmospheric CO_2 (Borges and Abril, 2011; Cloern et al., 2014). The Land-Ocean Interactions in the Coastal Zone Program (LOICZ) budgetary assertions of more than 250 estuaries and lagoons have also shown that most of them are heterotrophic or may have a balanced metabolism (Knoppers, 1994; Smith et al., 2010). CO_2 outgassing in most sectors of the estuaries is supported by the inputs of CO_2-enriched freshwaters, and by the CO_2 generated in the estuarine system itself, planktonic and benthic net heterotrophy and CO_2 advection from saltmarshes and mangroves (*e.g.* Borges and Abril, 2011; Cai, 2011). On the other hand, low pCO_2 waters and autotrophic metabolism has been observed in some estuarine plumes but with a small percentage of the surface area when compared to the freshwater influence (Borges and Abril, 2011). As more systems are being included in the budgeting effort, the global estuarine CO_2 emission estimate at the air-water interface has been declining (Borges and Abril, 2011; Guo et al., 2012; Chen et al., 2013; Huang et al 2015). The pioneer estimate of the CO_2 released by estuaries was 0.51 Pg C yr^{-1} (Borges, 2005) and the latest estimate has been adjusted to 0.094 Pg C yr^{-1}. (Chen et al., 2013). In fact, first budgets were based on data in systems generally located at temperate regions, being river-dominated, macrotidal and turbid (Borges, 2005; Borges and Abril, 2011). The more recent estimate includes a set of new data from estuaries located at low wind regions and the Arctic Ocean, which contributed to the decrease of the carbon released (Chen et al., 2013). Additionally, Jiang et al. (2008) demonstrated that pCO_2 can be significantly lower in marine-dominated estuaries than river-dominated, and according to Maher and Eyre (2012) marine dominated estuaries with low freshwater influences can be CO_2 sink.

In tropical regions, the spatial coverage of CO_2 fluxes of estuaries is still scarce. However, the limited number of available studies suggest that tropical estuaries are generally sources of CO_2 to the atmosphere (Souza et al., 2009; Sarma et al., 2012; Araujo et al., 2014), except for one lagoon (Koné et al., 2009). Also, most studies are potentially biased by the lack of information on the diurnal variations of CO_2, which corresponds to a crucial component of mass balance calculations (Borges and Frankignoulle, 1999; Zhang et al., 2013; Maher et al., 2015).

The CO_2 budgets of coastal ecosystems may also be altered by eutrophication generated by the anthropogenic nutrient inputs from sewage and fertilizer usage in agriculture, which has become a widespread water quality issue (Nixon, 1995; Cloern, 2001). The consequences of eutrophication, like the development of excessive algal blooms, toxic algae, loss of submerged aquatic vegetation and increase of hypoxia and anoxia, has been well documented (Bricker et al., 2003; Rabalais et al., 2009). However, the influence of eutrophication *per se* on the CO_2 budgets is poorly documented. In fact, the response of estuarine metabolism to eutrophication seems to be system type-specific. Some papers discussed that eutrophication can amplify autotrophy and favour CO_2 uptake (Gypens et al., 2009), while others show that eutrophication can reinforce heterotrophy and CO_2 degassing (Sarma et al., 2012; Chou et al., 2013; Wallace et al., 2014).

The present study addresses the question whether a tropical, marine-dominated, and eutrophic estuarine system Guanabara Bay (SE-Brazil) is a sink or a source of atmospheric CO_2. The bay, surrounded by the City of Rio de Janeiro, is the second largest Brazilian estuarine embayment (Kjerfve et al., 1997). The system is one of the most degraded estuaries worldwide. The waters of Guanabara are eutrophic to hypertrophic (according to the classification of Nixon, 1995) and provide ideal conditions to assess the response of aquatic CO_2 metabolism under marked eutrophication. CO_2 fluxes at the air-water interface of Guanabara Bay were estimated with continuous monitoring of surface water pCO_2, taking into account different temporal (daily and seasonal) and spatial scales. Our results show a very different behaviour in terms of carbon cycling of Guanabara Bay compared to previously documented estuaries, with extremely low values of pCO_2 and a net uptake of atmospheric CO_2 annually.

2 Material and Methods

2.1 Study Site

Guanabara Bay (22°41’ - 22°58’ S and 43°02’ - 43°18’ W) is located at the SE-Brazil coast, SW-Atlantic, and embedded within the metropolitan area of Rio de Janeiro, the second most densely populated region of the Brazilian Coast (Fig. 1). The bay has a surface area of 384 km^2, a mean depth of about 5.7 m, and a volume of 1870 x 10^6 m^3. The main subaqueous channel runs from the bay´s 1.8 km wide entrance with depths varying from 25 to 50 m up to 6 km inwards and along 24 km to the upper 20 km wide bay, with depths down to about 2 to 3 m. The lateral portions of the bay are spiked by small bays, with depths of about 2 m. It is a partially mixed estuarine embayment (Kjerfve et al., 1997), being completely mixed in wintertime but can exhibit stratified conditions in summertime due to concomitant effects of sunlight (thermal stratification) and freshwater discharge (haline stratification) mostly in the central and inner regions (Bérgamo, 2010).

The Bay is subject to a semi-diurnal microtidal regime with an annual mean of 0.7 m and spring tides attaining 1.3 m. With the exception of the entrances of small rivers, salinities vary between 25 and 34. The time for renewal of 50% of the total water volume is 11.4 days and water circulation is complex, as currents are modulated by tide and abrupt changes in the geomorphological configuration (Kjerfve et al., 1997). Circulation between the central and upper western regions is hampered by the presence of a large island (Ilha do Governador, Fig. 1). At the bay´s mouth, maximum water velocities vary between 0.8 – 1.5 m s^{-1} and seawater residence time is much shorter than in most inner regions, particularly behind Governador Island, where maximum current velocities are less than 0.3 m s^{-1} (Kjerfve et al., 1997).

Guanabara Bay is located in the intertropical zone and its climate is subject to variability of both the annual temperature and precipitation regimes. The weather is tropical humid (Bidone and Lacerda, 2004), with a warm and wet summer in October-March, and a cooler and drier winter in April-November. The most frequent winds in the bay from the N and NE in spring and summer, with monthly average velocity of 5 m s^{-1}. Winds from

the S and SE are associated with polar cold weather fronts being more common in autumn and winter (Amarante et al., 2002).

The drainage basin has an area of 4080 km^2 and includes 35 small rivers and streams, 6 of which flow into the upper region of the bay and contribute with up to 85% of the total runoff to the bay. The average annual freshwater water discharge to the bay is 100 ± 59 $m^3 s^{-1}$ and ranges from around 40 $m^3 s^{-1}$ in winter to 190 $m^3 s^{-1}$ in summer. Annual freshwater discharge is nine times smaller than the bay´s volume, which also contributes to the two-layered gravitational circulation (the ebb-flood oscillatory tidal current), resulting in the predominant saline (i.e. polyhaline) character of the waters (Kjerfve et al., 1997).

More than 7 million inhabitants discharge 25 $m^3 s^{-1}$ of untreated domestic wastewaters into the bay (Kjerfve et al., 1997; Bidone and Lacerda, 2004), which contributes to a load of about 465 T day^{-1} of organic matter (FEEMA, 1998). Small channels directly connected to sewage outlets are totally anoxic, but represent less than 5% of the surface area of the Bay. More intense cultural eutrophication since the 50´s (Borges et al., 2009) also contributed to hypoxic conditions of bottom waters in some of the more confined lateral and upper regions of the bay (Paranhos et al., 1998, Ribeiro and Kjerfve, 2002). Fluxes of phosphorous are currently 9-times higher than those estimated since the late 1800s (Borges et al., 2009). According to Godoy et al. (1998), sedimentation rates have increased up to 14 times over the last 50 years, in parallel with a 10-fold increase in the flux of organic matter to the sediments (Carreira et al., 2002).

In this study, five sectors were defined for the treatment, computations and interpretation of the data (Fig. 1): Sector one (S1) corresponds to the region up to 3 km inwards from the narrow and deeper tidal channel, is characterized by a maximum of seawater exchange, material dispersion and is partially mixed. Sector two (S2), located towards the western part of the bay, is delimited on the north by the Governador Island, which creates a barrier for direct tidal advection of waters into the upper north-western area of the bay. It is one of the most contaminated areas of Guanabara Bay. Sector three (S3) corresponds to the deeper channel which connects S1 (i.e. the bay's outlet to the South Atlantic) with the upper region. Sector four (S4) in the upper northeastern part of the bay, is shallow,

moderately impacted and bordered by 90 km^2 of mangrove forest and non-urbanized land. Sector five (S5) is the most confined area of the bay, located at the northwest and behind Ilha do Governador. It is shallow, has the longest residence time of waters and also receives significant amounts of sewage waters. The small western channel connecting S2 and S5 was disregarded from our analysis, due to its difficult access and extreme degree of contamination. However, it only covers less than 10 % of the entire sampled area.

2.2 Sampling Strategy

Nine sampling campaigns were performed with a frequency varying between 30 to 45 days from April 2013 to April 2014. Each campaign consisted in continuous measurements of the partial pressure of CO_2 (pCO_2), salinity, temperature, Chl *a*, DO, pH and GPS position, all at a frequency of 1 minute. Sub-surface (~30cm) water was pumped alongside the boat. In addition to the spatial screening, the diurnal variations of water pCO_2 were estimated on four occasions within the upper and most eutrophic sectors (S4 and S5) and also once in S1, by performing lateral trajectories forth and back across the sectors from dawn (04:30 am) to afternoon or dusk (at the latest until 09:30 pm). Diurnal measurements were made in Aug. 2013 and Jan. 2014, Feb. and Apr. 2014 (S4 and S5) and in S1 in Apr. 2014.

In addition, discrete sampling was performed at 16 to 19 stations along the continuous tracks (Fig. 1), except in Dec. 2013, when only 8 stations could be sampled due to logistical problems. Water samples were collected in sub-surface waters at a ~30cm depth with a Niskin bottle, and then conditioned (i.e. fixed and/or kept on ice in the dark) for further chemical analysis in the laboratory. Vertical profiles of temperature, salinity, fluorescence and DO were performed at all discrete stations with an YSI 6600 V2 multiparameter probe.

2.3 Analytical Procedures

2.3.1 Discrete parameters

Total alkalinity (TA) was determined on 100 ml filtrate from GF/F filtered samples, using the classical Gran (1952) electro-titration method by an automated titration system

(Metler Toledo Mod. T50). The reproducibility of TA was 4 μmol kg^{-1} (n=7). Measurements were compared to certified reference material (CRM provided by A.G. Dickson from Scripps Institution of Oceanography) and consistent at a maximum precision level of ±7 μmol kg^{-1}. Dissolved inorganic nitrogen (ammonia, nitrite, and nitrate) and phosphate were quantified as in Grasshof et al. (1999) and Chl *a* as in Strickland and Parsons (1972). Whatman GF/F filters were used for the Chl *a* analyses and the filtrate for the nutrient analyses. All water samples were kept in the dark and on ice during transport to the respective laboratories and nutrient samples and Chl *a* filters kept at −18 °C in a freezer prior to analyses.

2.3.2 On-Line parameters

Continuous measurements of temperature, salinity, fluorescence and DO were performed with a calibrated YSI 6600 V2 multiparameter probe inserted in a flow-through customized acrylic chamber. The values of the fluorescence sensor were correlated with the discrete analysis of Chl *a* to derive a conversion factor. pH was measured continuously with a pH-meter WTW 3310, equipped with a Sentix 41 electrode which was also inserted in the chamber, and calibrated with a three-point standard (pH 4.01, pH 7.00 and pH 10.01) according to the National Bureau Standard (NBS), before each sampling campaign. The precision of the pH measurements was about 0.01 (after 7 verifications against standards). As we have over determined the carbonate system (pCO_2, pH, and TA), we have chosen to use direct pCO_2 measurements and TA to calculate DIC. The pH measurements only served for a quality check. pCO_2 was measured using the marble-type equilibrator method, through which seawater flowed (1-2 L min^{-1}) from the top to the bottom of the cylinder filled with marbles and air was pumped upwards (1 L min^{-1}) (Frankignoulle et al., 2001; Abril et al., 2006). The air in the equilibrator was dried before passing to a non-dispersive infrared gas analyser (LICOR®, Type LI-820). We used three gas mixture standards (pCO_2 of 410, 1007 and 5035 ppmv) to calibrate the LICOR before each sampling (White Martins Certified Material, RJ, Brazil). We used N_2 passing through fresh soda lime to set the zero, and we used the standard at 1007 ppmv to set the span. We used the 410 and 5035 ppmv standards to check for linearity. The number of verifications after each calibration was about 7. The LICOR signal was stable and linear in the range of calibration and observations in the field (0-5000 ppmv). We also verified the drift before and after each sampling campaign. The partial pressure of atmospheric

CO_2 was measured in dry air twice a day, at the start and the end of the continuous runs. The precision and the accuracy of the pCO_2 measurements were about 3 and 5 ppmv, respectively.

Solar radiation, wind velocity (U10), accumulated precipitation and atmospheric temperature were recorded in the meteorological stations of Santos Dumont and Galeão airports (red squares in Fig. 1) and were provided by Brazilian Institute of Aerial Space Control (ICEA). The data sets of solar radiation (Rs) were converted into daily-averaged photosynthetically active radiation (PAR) using a conversion factor PAR/Rs of 0.5 (Monteith, 1977).

2.3.3 Calculations

2.3.3.1 The Carbonate System

Dissolved inorganic carbon (DIC) was calculated using two different pairs of measured parameters: pCO_2/TA and pH/TA using the carbonic acid constants sets proposed by Mehrbach et al. (1973) refitted by Dickson and Millero (1987), the borate acidity constant from Lee et al. (2010) and the CO_2 solubility coefficient of Weiss (1974). Calculations were performed in the CO2calc 1.2.9 program (Robbins et al., 2010). Both calculations gave very consistent DIC concentrations at ± 6.5 μmol kg^{-1}. DIC calculated from pCO_2/TA and pH/TA pairs gave an excellent agreement (slope: 1.008, R^2=0.995). The slope was not statistically different from 1 ($p = 0.20$) and the intercept was not significantly different from 0 ($p = 0.86$). The excess of DIC (E-DIC, μmol kg^{-1}) was calculated as the difference between the in-situ DIC (DIC in situ μmol kg^{-1}) and a theoretical DIC at atmospheric equilibrium (DIC equilibrium μmol kg^{-1}) according to Abril et al. (2003). The DIC equilibrium was calculated from observed TA and the atmospheric pCO_2 measured in the Bay. The apparent oxygen utilization (AOU, μmol kg^{-1}) was calculated from the temperature, salinity and DO concentrations measured continuously with the probe and the theoretical DO saturation (Benson and Krause, 1984).

Diffusive air-sea CO_2 fluxes were computed from pCO_2 measured in the water and the atmosphere and a gas transfer velocity derived from wind and other physical drivers. We used the k-wind parameterization of Raymond and Cole (2001) and Abril et al. (2009), which are gas exchange coefficients specific for estuarine waters. The Raymond and Cole

(2001) (RC01) equation is based on the compilation of gas transfer velocities derived from tracers applied to nine rivers and estuaries, using only wind speed as an entry parameter. The Abril et al. (2009) (A09) relationship is based on chamber flux measurements in seven estuaries, and uses wind speed, estuarine surface area, and water current velocity as entry parameters. We also calculated the fluxes with the parameterization of Wanninkhof (1992) (W92), which was initially developed for open ocean waters. The gas transfer coefficients normalized to a Schmidt number of 600 obtained with the three parameterizations were then converted to the gas transfer velocity of CO_2 at *in situ* temperature and salinity following the procedure of Jähne et al. (1987). Fluxes were computed for each sector of Guanabara Bay, using water pCO_2 representative for diurnal and seasonal variations.

2.3.3.2 The Net Community Production (NCP)

The NCP was calculated by the changes in dissolved inorganic carbon (DIC) obtained from a set of lateral trajectories performed forth and back from dawn to dusk. As such, sampling addressed different times of the day at similar locations and NCP was computed from the diurnal DIC variations according to the following equation:

$$NCP = ((DIC_1 – DIC_2)\rho d)/\Delta t – FCO_2 \quad (1)$$

where NCP is the net community production (mmol m^{-2} h^{1}), DIC_1 and DIC_2 represents the salinity-normalized concentration of dissolved inorganic carbon (mmol kg^{-1}) during two consecutive trajectories (from dawn to dusk), ρ is the seawater density (kg m^{-3}), d is the average depth (m) of the area, t represents the time interval (hours) and F is the carbon dioxide flux (mmol m^{-2} h^{-1}) across the water-atmosphere interface. The computations were carried out with the mean values of DIC during each trajectory.

2.3.3.3 Temperature and biological effect on pCO2 variations

The temperature *versus* biological effect on pCO_2 variations in Guanabara Bay was verified using the Takahashi et al. (2002) approach. The relative importance of the temperature and biological effects can be expressed as a ratio between both the temperature and the biology effect. The biological component is estimated by the seasonal amplitude of the temperature-normalized pCO_2 and the temperature component is characterized by the seasonal amplitude of the annual mean pCO_2 corrected for the seasonal temperature variation. The following equations were applied (Takahashi et al., 2002):

pCO_2 at T_{mean} = pCO_{2obs} x exp[0.0423(T_{mean}-T_{obs})] (variations driven by biological effect); (2)

pCO_2 at T_{obs} = pCO_{2mean} x exp[0.0423(T_{obs}-T_{mean})] (variations driven by thermodynamic effect); (3)

where T is the temperature in ^{o}C, and the subscripts ‘‘mean’’ and‘‘obs ’’ indicate the annual average and observed values, respectively. These equations were applied to summer and winter conditions as a whole. The biologic effect on the surface-water pCO_2 (ΔpCO_2)Bio is represented by the seasonal amplitude of pCO_2 values corrected by the mean annual temperature, (pCO_2 at T_{mean}), using Eq. (1):

(ΔpCO_2)Bio = (pCO_2 at T_{mean})$_{max}$ – (pCO_2 at T_{mean})$_{min}$; (4)

where the subscripts ‘‘max’’ and ‘‘min’’ indicate the seasonal maximum and minimum values. The effect of temperature changes on the mean annual pCO_2 value, (ΔpCO_2)temp, is represented by the seasonal amplitude of (pCO_2 at T_{obs}) values computed using Eq. (2):

(ΔpCO_2)Temp = (pCO_2 at T_{obs})$_{max}$ – (pCO_2 at T_{obs})$_{min}$; (5)

A ratio (ΔpCO_2)Temp/(ΔpCO_2)Bio (Temp/Bio) > 1 indicates a dominance of the temperature effect over mean annual pCO2 values, whereas a ratio < 1 indicates dominance of a biological effect (Takahashi et al., 2002).

2.4 Statistical Analysis

Normality test was carried with the Shapiro-Wilk test. If the data showed parametric distribution, we used t-test to comparing averages. If the data showed non-parametric distribution, we used the Mann-Whitney test. The calculations of correlations between variables were performed with the Spearman rank coefficient. Simple linear regressions were calculated to compare calculated and measured variables (DIC and pH), and the comparison between slopes was made with one test equivalent to an Analysis of Covariance (ANCOVA). For the principal component analysis (PCA) calculation, the sampling campaigns were taken as cases, and the parameters were taken as variables. The PCA technique starts with a correlation matrix presenting the dispersion of the original variables (data were normalized by z-scores with average data for each sampling campaign), utilized for extracting the eigenvalues and eigenvectors. Henceforth, the principal components were obtained by multiplying an eigenvector by the original

correlated variables. All statistical analysis were based on $\alpha = 0.05$. We utilized the Statistic 7.0 program to perform all PCA steps and the GraphPad Prism 6 program to perform the other statistical tests.

3 Results

3.1. Climatic, hydrological and biogeochemical conditions

Climatic conditions during the study period followed a classical seasonal trend (Fig. 2), with exception of Jan. 2014 and Feb. 2014, when the air temperature was warmer (2.2 °C higher, $p < 0.001$, t-test) than the averaged reference period of 60 years (1951-2010). The other sampled months had air temperature and precipitation consistent with historical data (Fig. 2), despite of some deviations from the historical average especially for accumulated precipitation. Sector-averaged surface water temperature in Guanabara Bay (Table 1) varied between 23.8 and 26.8 °C and salinity varied between 27.0 and 32.2. In the upper portion of the bay (S4 and S5), salinity decreased in winter and temperature increased in summer with an observed maximum of 33.9 °C. S1, at the entrance of the bay, exhibited lowest temperatures and highest salinities, with little seasonal variation. A maximum seasonal amplitude of 3.4 °C and 2.8 °C of sector-average temperature occurred in S4 and S5, respectively. When considering sector-averaged values, seasonal contrasts were less than 2 salinity units in all sectors. Spatially, the most confined northern sectors which receive more river water, showed the lowest salinity, particularly at the vicinity of river mouths, and during the rainy season, with a minimum of 14.6 in Apr. 2013 in S4.

Average values for pH, TA, DIC, Chl *a* and nutrient data reported for each sector in Table 1 reflect the eutrophic (S1 and S3) to hypertrophic (S2, S4 and S5) conditions prevailing in Guanabara Bay, consistent with previous works (Rebello et al., 1988; Ribeiro and Kjerve, 2001). All water quality parameters (nutrients and Chl *a*) exhibited a large standard deviation (SD) to the mean. Ammonium (NH_4-N) was the dominant form of dissolved inorganic nitrogen (DIN) and reached average concentrations of around 45 and 27 µM in S2 and S5 and 8, 9 and 5 µM in sectors S1, S3 and S4, respectively. The maximum range was recorded in S5 (0.13 to 130 µM NH_4-N) and the minimum range in the lower S1 (8.15 to 22.5 µM NH_4-N).

Extremely high Chl *a* values were associated with high pH and moderately to low nutrient concentrations, indicating that nutrients were fixed into phytoplankton biomass. Average Chl *a* concentrations followed the trophic state gradient, increasing from the mouth of the bay toward its upper portion and also in the lateral embayments (Table 1). All sectors showed high spatial and temporal variability of Chl *a*. In general, highest values were recorded during summer conditions and lower values during winter. This feature has also been observed by other studies (Guenther et al., 2008; Guenther et al., 2012). Sectors 3, 4 and 5 experienced the densest phytoplankton blooms, Chl *a* reaching maxima on one occasion of 537 µg L^{-1} in S3, 289 µg L^{-1} in S4 and 822 µg L^{-1} in S5.

3.2 Vertical structure of the water column

The vertical profiles for temperature, salinity, DO and Chl *a* in S1, S3 and S5, shown in Figure 3 are well representative of other observations in the outer, middle and inner regions of Guanabara Bay, both for summer and winter conditions. During winter, the water column was well mixed in all sectors. Indeed, temperature and salinity showed little vertical variations during this season (Figs. 3a, 3c and 3e). Chl *a* and oxygen profiles were also vertically homogeneous, except in the most confined and shallow S5, where Chl *a* was typically 2.5 times higher in the first two meters compared to the bottom (Fig. 3f). During summer, all sectors showed important thermal and saline stratification (Figs. 3g, 3i and 3k), halocline and thermocline being located almost at the same depth. In 20m-deep water columns (S1 and S3; Figs. 3g and 3i), a ~4m deep surface layer was ~2-3°C warmer and had salinity ~1-2 units lower than the bottom layer; in 5m-deep water column (S5; Fig. 3k), the warmer surface layer was ~2m deep with similar temperature and salinity contrasts between the surface and the bottom. The vertical water profile was also analysed to investigate the diurnal variations of temperature and salinity (Figs. 3k and 3l). Comparison between daytime and nighttime conditions revealed that stratification was subject to diurnal variations, driven by temperature convection concomitant with a moderate mixing of water currents by microtidal action. Summer stratification of the water column was accompanied by a consistent vertical distribution of Chl *a* and oxygen, with maximum in the surface layers and minimum at the bottom. Note that the salinity varied less than the temperature along the day (> 2°C of variation in 5 hours; Fig. 3K). Stratification apparently favoured phytoplankton development, as Chl *a* concentrations were highest (up to 240 µg L^{-1}) at the surface of the stratified water columns. These

physical conditions were largely predominant in summer and in the shallowest, calmest and most confined sectors of the Bay (S4 and S5).

3.3 Spatial distributions of pCO_2 in surface waters

Spatial distributions of surface water pCO_2 measured continuously along the trajectories, revealed strong spatial gradients between and/or inside each sector, from over- to under-saturation with respect to the atmosphere (Fig. 4). Temporally and spatially, water pCO_2 was inversely correlated with dissolved oxygen (R^2= -0.88; n=9002; $p < 0.0001$) and Chl *a* (R^2= -0.54; n=9004; $p < 0.0001$). S1 presented pCO_2 values close to the atmospheric equilibrium, with moderate temporal variation around this average (411±145 ppmv). DO and Chl. *a* in S1 were 103±29 % and 19±22 μg L^{-1}, respectively. S2, close to most urbanized area, showed highest heterogeneity, from a maximum pCO_2 value of 3750 ppmv in hypoxic waters (DO=2% saturation) at the vicinity of the highly polluted urban channels in Jan. 2014 (Fig. 4g), to strong undersaturation, as low as 50 ppmv related to a bloom formation (Chl. *a* = 212 μg L^{-1}) in Jan.2014. In S2, the extent of pCO_2 supersaturation apparently induced by the urban sewage loads was favoured by strong rains the day before sampling and low PAR incidence in Jul., Aug. and Sep. 2013, compared to all the other cruises (Fig. 4). In S3, S4 and S5, which account for 75% of the surface sampled area of Guanabara Bay, pCO_2 was predominantly below the atmospheric equilibrium, particularly during daytime summer cruises (Fig. 4 and Table 1). Massive phytoplankton blooms were sampled during our survey, characterized by extreme patchiness in summer. For example, an extreme of 22 ppmv of pCO_2, 350 % sat DO and 550 μg L^{-1} Chl *a* was recorded in Feb. 2014 in a brown/red bloom. In S3, S4 and S5, water pCO_2 was lower than 150 ppmv around midday at all seasons. These blooms and associated pCO_2 under-saturation occurred in S4 and S5 during winter and progressively spread to the entire bay during summer months (Fig. 4). From Sep. 2013 to Feb. 2014, midday undersaturation was encountered over the whole bay, except the urban impacted S2 (Fig. 4). Finally, some increases in water pCO_2 above the atmospheric equilibrium (up to a maximum of 2200 ppmv) were observed in Jul. 2013, Aug. 2013 and Apr. 2014, in the northeastern part of S4 and S5, related to river plumes. Before reaching the bay waters of S4, these riverine plumes flowed across a preserved mangrove area. However, the extent of these small plumes was limited (Fig. 4) and their contribution to the sector CO_2 balance was apparently negligible.

3.4 pCO_2 diurnal variations

The five back and forth tracks revealed important diurnal changes in water pCO_2 in S4 and S5, but not in S1 (Fig. 5). In the S1 in Feb.2014 (Fig. 5d), nighttime (predawn) pCO_2 (451 ± 38 ppmv) was not significantly different ($p > 0.05$ Mann-Whitney Test) from daytime pCO_2 (466 ± 26 ppmv). In contrast, in S4 and S5, rapid and significant decreases in water pCO_2 were recorded in the early hours of the morning, followed by a relatively stable undersaturation from 10:00 AM to all over the afternoon (Fig. 5). For instance, in Sep. 2014, pCO_2 decreased from 800 ppmv at 8:30 AM to 200 ppmv at 13:40 PM at the same geographical location (Fig. 5a). The decrease in water pCO_2 occurred relatively quick on all occasions at around 9:30 AM, which apparently corresponded to the hour of maximum photosynthetic activity by phytoplankton. 9:30 AM was then used as the limit to separate nighttime pCO_2 from daytime pCO_2. In S4 and S5, pCO_2 changes from nighttime to daytime were from 591 ± 231 to 194 ± 114 ppmv in Sep. 2013, from 163 ± 40 to 116 ± 25 ppmv in Jan. 2014, from 346 ± 166 to 146 ±106 ppmv in Fev. 2014, and from 637 ± 421 to 265 ± 186 ppmv in Apr. 2014. In all these cases, water pCO_2 was significantly higher ($p < 0.001$; Mann-Whitney Test) before than after 9:30 AM. Consequently, S4 and S5 shifted from a CO_2 source at nighttime to a CO_2 sink at daytime in Sep.2013 and Apr.2014, but remained a CO_2 sink all day and night long in Jan. and Feb. 2014. In addition to these five back and forth tracks described in Fig. 5, we could compare water pCO_2 values measured on the same day in the early morning (before 9:30 AM) with those measured in late afternoon in S1, S3 and S4. Consequently, our data provided a fairly good indication of the diurnal variability of pCO_2 throughout the entire sampling period, in all sectors, except S2 (Fig. 6).

3.5 Seasonal Variations

Clear seasonal changes were observed in pCO_2 of surface waters (Fig. 6), with higher values in winter (Apr. 2013, Jul. 2013, Aug. 2013, Sep. 2013 and Apr. 2014) than in summer (Oct. 2013, Dec. 2013, Jan. 2014 and Feb. 2014). Seasonal variations in DO and Chl. *a* mirrored the pCO_2 variations, with a maximum phytoplanktonic biomass and oxygen saturation in summer, when pCO_2 was at its minimum. S1 was a source of atmospheric CO_2 during winter (pCO_2 of 501 ± 98 ppmv), but a sink during summer

(pCO_2 of 304 ± 117 ppmv). S2 presented the highest pCO_2 differences between winter (923 ± 484 ppmv) and summer (423 ± 530 ppmv), with high standard deviations resulting from spatial heterogeneity for both periods (Fig. 4). In S3, S4 and S5, CO_2 undersaturation prevailed along the year, except in winter and nighttime, where oversaturations prevailed. In these three sectors, oxygen remained oversaturated all over the year. Average measured values of pCO_2 for winter and summer respectively, were 353 ± 141 and 194 ± 127 in S3, 380 ± 286 and 203 ± 159 in S4, and 364 ± 343 and 132 ± 74 ppmv in S5. Note that these averages are in its majority based on daytime measurements and that integrated yearly average CO_2 fluxes had to be quantified by accounting for both seasonal and diurnal variations (see following section and discussion).

3.6 Gas transfer velocities, CO_2 fluxes at the air-sea interface and NCP

Wind speeds (12h-averaged) varied between 1.4 and 3.9 m s^{-1}, were significantly higher during summer than during winter ($p < 0.001$; t-test) and significantly higher during daytime than during nighttime ($p < 0.001$; t-test) (Table 2). Instantaneous wind speed showed some peaks at a maximum of 15 m s^{-1} during short (<1h) events. Wind speeds measured at the meteorological station in the southern part of the Bay were higher (S1, S2 and S3) than those recorded at the station in the northern region (S4 and S5) (Table 2).

Calculated gas transfer velocities averaged over daytime and nighttime periods varied between 0.8 and 12.3 cm h^{-1} (Table 2). k_{600} values calculated from the equation of Abril et al. (2009) that accounts for the wind velocity, the fetch effect linked to estuarine size and the current velocity, was systematically higher than those calculated from the relationships of Raymond and Cole (2001) and Wannikhof (1992), which consists in exponential functions of wind velocity, with the former being specific for estuarine waters and the latter primarily developed for open ocean waters. Average k_{600} values based on 15min wind speed were not significantly different from k_{600} based on 12h average wind speed, showing that short storms had negligible impact on daily-integrated gas transfer velocities. CO_2 fluxes were calculated using the measured pCO_2 in each sector during the respective period: summer and winter, daytime and night-time. In the absence of data, we interpolated pCO_2 from surrounding areas and/or measurement periods. For S2, the only

sector that was not sampled at night, we applied the mean diurnal variations of S1 and S3. Because of the relatively narrow range of k_{600} variation, calculated CO_2 fluxes followed the pattern of surface water pCO_2 and varied between 14.6 mmol m^{-2} h^{-1} in the polluted S2 during winter and nighttime, to -9.7 mmol m^{-2} h^{-1} in dense phytoplanktonic blooms of S5 during summer and daytime (Table 2). Time-integrated CO_2 fluxes, accounting for seasonal and daily variations, revealed that all sectors except S2 behaved as CO_2 sinks on an annual basis.

The NCP estimates to Guanabara Bay encompassed four sampling campaigns (Sep. 2013, Jan. 2014, Feb. 2014 and Apr. 2014). The values ranged between 51 to 255 mmol m^{-2} d^{-1}, with an annual average of 143 ± 56 mmol m^{-2} d^{-1}. The summertime period presented an average of 161 ± 49 mmol m^{-2} d^{-1}, whereas for wintertime the NCP was 126 ± 51 mmol m^{-2} d^{-1}. All values of NCP were positive indicating that upper sectors of Guanabara Bay were autotrophic.

4. Discussion

4.1 Estuarine Typology: Comparing Guanabara Bay with other estuaries

The results of the continuous measurements and the concomitant discrete sampling of water quality parameters, showed that, in terms of CO_2 atmospheric exchange, Guanabara Bay does not follow the patterns of a typical drowned-river valley estuary with a marked longitudinal estuarine gradient between its fresh and marine water end-member sources (Pritchard, 1952). Rather, Guanabara Bay corresponds to a tropical marine dominated system, owing to the small freshwater discharge relative to its water volume and tidal exchange, maintaining 85 % of the bay with salinities always higher than 25. Its geomorphological characteristics and rather complex circulation of water masses, makes the application of standard approaches to discern sources or sinks from composite plots between salinity and material concentrations difficult (Bourton and Liss, 1976). Furthermore, Guanabara Bay has been considered as one of the world´s most degraded embayment characterized by constant eutrophic to hypertrophic conditions and the frequent occurrence of red tides (Rebello et al., 1988; Villac and Tennenbaum, 2010; Guenther et al., 2012).

The CO_2 behavior in Guanabara Bay was different from that in most of documented estuaries worldwide. Indeed, the majority of studies that were conducted in macrotidal, turbid and river-dominated estuaries reveal that these systems are heterotrophic and emit large amounts of CO_2 both in temperate and tropical regions (Frankignoulle et al., 1998; Borges and Abril, 2011; Sarma et al., 2012). These drowned valley, river-dominated, estuaries also exhibited a significant inverse trend between salinity and pCO_2 (Frankignoulle et al., 1998), which was not observed in Guanabara Bay. The absence of a negative relationship between pCO_2 and salinity for the range of 27 to 32 is in fact more consistent with observations in some estuarine plumes (although less pronounced), where pCO_2 undersaturation and diurnal variations are often reported (Borges and Frankignoulle, 1999; Borges and Frankignoulle, 2002; Dai et al., 2009; Bozec et al., 2011). Therefore, our results in Guanabara Bay are still consistent with the comparative analysis of CO_2 dynamics in river- and marine-dominated estuaries by Jiang et al. (2008). In Guanabara Bay, salinities lower than 27 were confined to the upper region at the mouths of the small rivers in S4 (max. pCO_2 = 2222 ppmv), S5 (max. pCO_2 = 2203 ppmv) and some polluted channels of S2 (max. pCO_2 = 3715 ppmv) (Table 1 and Fig. 4). However, these heterotrophic and strong CO_2 degassing regions are relatively small when compared to the total surface area. In contrast, pCO_2 in S1, which is directly affected by marine water intrusion, exhibited minor diurnal and seasonal variations oscillating around the atmospheric value of 400 ppmv. But, sectors 3, 4 and 5 as a whole, which cover around 75 % of the bay´s area, behaved as a net CO_2 sink on an annual basis, with concentrations even down to about 30 ppmv on some occasions (Table 2). These three sectors are subject to weaker tidal currents, higher water residence times, and stratification at shallow depths, favouring CO_2 uptake by phytoplankton primary production and autotrophic metabolism, especially during summer. Indeed, thermal or haline stratification of estuarine waters has been identified as a determinant factor that favours the ecosystem to act as a CO_2 sink (Borges 2005; Chou et al., 2013). Low pCO_2 values at surface waters were reported for the inner shelf of the Changjiang estuary (Chou et al., 2013), the outer Loire estuary (Bozec et al., 2012), the lower Pearl River estuary (Dai et al., 2008), the Amazon river plume (Körtzinger, 2003) and on the Mississippi River-dominated continental shelf (Huang et al., 2015), all with enhancement of stratification stimulating phytoplankton bloom development and uptake of CO_2. Low pCO_2 values were also observed in estuaries which receive low freshwater discharge and present low water exchange with the sea (Jiang et al., 2008; Koné et al., 2009; Maher and Eyre, 2012; Sarma et al., 2012).

The comparison of the E-DIC versus AOU values (Fig. 7) from our study with a compilation of data obtained for 24 estuaries, in majority river-dominated estuaries located in temperate regions (Borges and Abril, 2011) illustrates the specific metabolic characteristics of Guanabara Bay. The negative E-DIC and AOU values found for Guanabara Bay suggest the system is autotrophic. The 1:1 line represents the quotient between CO_2 and O_2 during planktonic primary production and community respiration (Borges and Abril 2011). The values close along this line for Guanabara Bay suggest that gross primary production and total (autotrophic and heterotrophic) respiration are coupled, and largely dominated the signal, with a strong biological control on the production/consumption of these gases. Many data from other estuaries are situated well above the 1:1 line, especially at high pCO_2 values, indicating lateral inputs of dissolved CO_2 from tidal marshes or mangroves, faster equilibration of oxygen with the atmosphere than carbon dioxide due to differences in solubility and the buffering capacity of the carbonate system, and/or anoxic respiration in sediments (Cai et al., 1999; Abril et al., 2002; Bouillon et al., 2008; Borges and Abril, 2011). In Guanabara Bay, mangrove forests are not so extended, and the volume of water exchanged with the mangrove sediments is moderate due to the modest tidal amplitude. For that reason, we could not find supersaturated pCO_2 conditions near of the mangrove region, at least at about 2km distance from the mangrove. This suggests that dissolved CO_2 export from the mangrove is low and probably associated with a rapid consumption of mangrove-derived DIC by the phytoplankton.

4.2 Meteorological and biological control of pCO_2 in Guanabara Bay

A PCA was performed to better identify the variable contributions of the data. For each sampling day, we calculated the mean values of pCO_2, DO, pH, Chl *a*, temperature, salinity, wind velocity, PAR incidence and also the seven days of accumulated precipitation. The PCA revealed a strong meteorological control on the pCO_2 dynamics in Guanabara Bay (Fig. 8). Factor 1 explains 65% of the total variance revealing that pCO_2 was well separated and negatively related to DO, Chl *a*, temperature, wind velocity and PAR incidence. This suggests a strong external meteorological control on phytoplankton dynamics and, in turn, on the CO_2, DO and Chl *a* at spatial and temporal scales. Indeed, the high incident light simultaneously provides energy for phytoplankton

growth and favors the development of thermal stratification, particularly in the shallow and less hydrodynamic regions (Fig. 3). In the tropics, high light incidence combined with the presence of nutrients contributes to phytoplankton blooms and CO_2 depletion both directly, by supplying light for photosynthesis, and indirectly by favoring stratification of the water column. It is noteworthy that high wind speed in the region of Guanabara was correlated with high PAR, and consequently, gas exchange was favored during daytime, when CO_2 depletion attained its maximum. In contrast, salinity and the 7-day accumulated precipitation were not related to the other parameters, and dominating the factor 2, that explain about 19% of the variance in the data. This suggests that pulsated inputs of freshwater, typical of tropical storms affects salinity in Guanabara Bay, but has little impact on the intensity of blooms and the CO_2 uptake by the phytoplankton.

Our diurnal measurements along the hypertrophic sectors 4 and 5 also showed marked differences of pCO_2 concentrations between daytime and nighttime. The nighttime pCO_2 values were about 30% higher than daytime (differing by up to 395 ppmv). As the PAR incidence increased along the day, the surface pCO_2 decreased due to the enhancement of photosynthesis and rapid formation of thermal stratification (Figs. 3 and 5). Our report of strong diurnal variation in pCO_2 in Guanabara Bay (Fig. 5) reveals how photosynthesis and respiration processes vary temporally, especially in areas with high phytoplankton biomass (indicated by Chl *a* values above 50, sometimes reaching 200 µg L^{-1}). In their study of primary production based on oxygen incubations in Guanabara Bay, Rebello et al. (1988) postulated that some intriguing very low rates in Chl *a* rich samples were due to the occurrence of CO_2 limitation. Indeed, the extremely low values of pCO_2 observed in S5 (ex. 24 ppm or 0.6 µmol kg^{-1} of dissolved CO_2) confirm that CO_2 might be one of the limiting factors for primary production. However, in such CO_2 limiting conditions, phytoplankton would need to take up bicarbonate using the proton pump mechanism and the carbonic anhydrase enzyme (Kirk, 2011). Some diurnal variations of pCO_2 controlled by biological activity have been reported in several other estuarine systems worldwide (Dai et al., 2009; Bozec et al., 2011; Yates et al., 2007; Zhang et al., 2013). In the Bay of Brest, a temperate coastal embayment, the phytoplankton blooms were responsible for 10 to 60% of the seasonal pCO_2 drawdown observed during spring, equivalent to 100-200 ppmv (Bozec et al., 2011). In Tampa Bay, a shallow subtropical estuary, the diurnal variations in pCO_2 (median of 218 ppmv) were largely influenced by primary productivity

and respiration of benthic communities (Yates et al. 2007). Also, Zhang et al. (2013) reported diurnal pCO_2 variations mainly controlled by biological activities (maximum 218 ppm in autumn) in a Chinese tropical open bay dominated by fringing reefs; however, calcification was also important driver of diurnal pCO_2 variations in winter. In one suite of different coastal ecosystems in the South China Sea, including inshore and onshore locations, Dai et al. (2009) concluded that temperature was a major driver of pCO_2 diurnal variability in the oligotrophic and offshore regions (10-16 ppmv variations), tidal effects in the nearshore (41-152 ppmv), and biological metabolism in the coral reef system (up to 608 ppmv of diurnal variations). Henceforth, it is clear that diurnal variations must be accounted for in estuarine CO_2 budget assertions, otherwise estimates based on daytime pCO_2 measurements only might shift the conclusions towards an overestimate of the CO_2 sink, or an underestimate of the CO_2 source. Henceforth, we use pCO_2 measurements at different hours of the day and night in order to integrate the diurnal variations.

The contributions of temperature and biological activity for Guanabara Bay were estimated at 33 and 255 ppmv, respectively, showing the strong influence of biological productivity upon pCO_2 dynamics in this tropical coastal embayment (ratio of 0.12). Some authors utilized the same approach in other estuarine systems with different dominances between temperature and the biological effect (Bozec et al., 2011; Zhang et al. 2012; Hunt et al., 2014). The temperature dominating effect was detected for Jiaozhou Bay (China Sea), Zhang et al. (2012) obtained pCO_2 variations differences of 93 and 78 ppmv for temperature and biological activity respectively (weak temperature prevalence and ratio of 1.19). In the Kennebec Estuary (USA), Hunt et al. (2014) found different rations according to the salinity zones and showed that, in general, higher ratios prevailed at low salinities (1.9-2.1), with higher temperature control on pCO_2 variations. Bozec et al. (2011), on the other hand, in one inter-annual approach encountered a mean value of 0.49, in the Bay of Brest, a temperate embayment in France, confirming that the biological processes were the main driver of the seasonal pCO_2 dynamic. The ratio for Guanabara Bay is much lower than in all these systems, and also consistent with an atypical CO_2 dynamics.

4.3 Eutrophication and CO_2 Dynamics

In several coastal systems worldwide, important CO_2 changes, either increasing or decreasing, have been attributed to eutrophication processes (Gypens et al., 2009; Borges and Gypens, 2010; Cai et al., 2011; Sunda and Cai, 2012; Chou et al., 2013). Eutrophication occurs when massive anthropogenic inputs of both organic (mainly domestic) and inorganic (agricultural or industrial) nutrients (sometimes during several decades) have enriched estuarine waters and sediments with bioavailable nitrogen and phosphorus (Rabalais et al., 2009). Increases in pCO_2 have been reported in river-dominated estuaries at the vicinity of megacities (Frankignoulle et al 1998; Zhai et al., 2007; Sarma et al., 2012). When sewage is discharged in such river-dominated systems, heterotrophy is enhanced and CO_2 outgassing increases (Zhai et al., 2007; Sarma et al., 2012). Indeed, environmental conditions in these turbid estuarine waters strongly limit primary production in favor of heterotrophy. Turbidity, together with stratification, is indeed a key parameter that explains pCO_2 variation in estuaries (Jiang et al. 2008; Borges and Abril 2011). In Guanabara Bay, sewage also predominates as source of organic nutrients (Bidone and Lacerda, 2004). However, the pCO_2 spatial distribution (Fig. 4) suggests that mineralization of this domestic organic matter occurs predominantly within the sewage network itself and in small rivers and channels and their plumes that represent a small surface area in the Bay. It can be noted for example that pCO_2 oversaturation was more extended in S2 in Aug. 2013, which corresponds to a sampling just after strong rains on the city of Rio de Janeiro. Mineralization of organic matter in these extremely polluted areas leads to rapid CO_2 (and probably CH_4) outgassing, and concomitantly, contributes to a long-term enrichment of the Bay in bioavailable nitrogen and phosphorus (Paranhos et al., 1998; Ribeiro and Kjerfve, 2002).

Except for these peripheral zones, most sectors of Guanabara Bay experienced massive algal blooms due to the optimal conditions for primary production, including nutrient, light, and water column stratification. The driving phytoplankton assemblages of Guanabara Bay are typical for eutrophic to hypertrophic systems, largely dominated by bloom and also red tide forming nanoplankton, filamentous cyanobacteria and some microplankton (Valentin et al., 1999; Santos et al., 2007; Villac and Tennenbaum, 2010). Preliminary investigations of the collected material from this study suggests that cyanobacteria were frequently encountered in S2, S4 and S5, during the 9 sampling periods, and great deal of patchiness was observed with a succession of intense red, brown

and/or green colored waters, leading to the marked short spatial variability of pCO_2, DO and Chl *a*. In the waters dominated by phytoplankton blooms the pCO_2 values were always extremely low, and the sink characteristics were prevalent, with high CO_2 uptake and autotrophy characteristics. It has been shown, that during summer the heterotrophic bacterial production (BP) lied within the range of only 0.4-19 % of primary production (PP) at the surface and 5-52 % at the bottom, being nutrient dependent (Guenther et al., 2008). Our spatial and temporal pCO_2 dataset (Fig. 4) also suggests that the most confined part of the inner bay apparently behaved as the "bloom genesis region" that can spread phytoplanktonic production, biomass, and associate CO_2 consumption over the rest of the estuarine system. Indeed, CO_2-depleted waters were confined to S4 and S5 in Oct. 2013, and progressively extended to all sectors (except S2) in Jan. 2014, During this period, conditions became ideal for bloom developments with increasing air and water temperature, and the development of water stratification (Figs. 4 and 6).

Eutrophication, thus enhances the low surface pCO_2 concentrations in Guanabara Bay. Phytoplankton uses more nutrients and dissolved CO_2 in the surface waters, and produce larger biomass of organic matter. When this additional material reaches the bottom, the organic matter and associated nutrients are recycled, increasing pCO_2 and decreasing the oxygenation of bottom waters (Fig. 3,k,l). Some authors recently discussed the increasing of bottom water acidification enhanced by coastal eutrophication especially in stratified ecosystems (Cai et al., 2011; Sunda and Cai, 2012). It has been shown, that water column stratification and bottom water stagnation enhances the isolation of O_2 and CO_2 in deeper waters and consequently their exchange between bottom and surface waters (Chen et al., 2007). Koné et al. (2009) reported a consistent CO_2 vertical distribution in Aby and Tendo lagoons, in Ivory Coast, where a warmer, fresher, Chl *a*-rich surface layer was depleted in CO_2 and nutrients, whereas a more saline and anoxic bottom layer was enriched in CO_2 and nutrients. Gypens et al. (2009) developed and validated a process-based model in the Scheldt estuary plume, that revealed that eutrophication could make the system shift from a net source of atmospheric CO_2 to a net sink, when anthropogenic nutrient loads increased, stimulating the carbon fixation by autotrophs. Chou et al. (2013) also suggested that human-induced increase in nutrient loading may have stimulated primary production and thus enhanced the CO_2 uptake capacity on the inner shelf off the Changjiang Estuary. Our results reveal that the impact of eutrophication on estuarine systems in terms of CO_2

exchange strongly depends on their typology. Drowned-valley, river-dominated, "funnel-type" estuaries, which are generally light-limited and heterotrophic, respond totally differently from estuarine plumes, marine-dominated lagoons or embayments like Guanabara Bay, where optimal condition for autotrophic primary production occur over large surface areas. These estuarine types are different in their hydrological and geomorphological configuration, availability of light, diversity of primary producer and heterotrophic assemblages, and their response to increasing nutrient loading (Smith et al. 2010; Cloern et al. 2004). Depending on the hydrodynamics, the additional organic carbon produced by enhanced eutrophication can be buried, mineralized, and/or exported. In quiescent embayments like Guanabara Bay, long-term burial can be significant (Carreira et al., 2002), resulting in a net uptake and storage of atmospheric carbon within the ecosystem.

4.4 Air-Water CO_2 Fluxes in Guanabara Bay

The spatial and temporal CO_2 fluxes were integrated for the Bay, taking into account the diurnal and seasonal variations of pCO_2, wind speed, and gas exchange coefficients. Efforts were made to sample all the sectors of the bay with different PAR intensities (higher, medium and low intensity, for each sampling day and especially in the more eutrophic waters). Characteristic daytime and nighttime pCO_2 where deduced from the five back and forth observations in S4 and S5, and from the comparison of early morning (before 9:30 AM) pCO_2 data with late afternoon data in S1, S3 and S4. Compared to seasonal changes, diurnal changes were significant, surface pCO_2 sometimes shifted from a sink behavior in the evening to source behavior at the end of the night, or sometimes remained under-saturated all night long (Fig. 6). Except for S2, the more polluted sector, and the only one acting as a CO_2 source, our data could be used to integrate diurnal variability of pCO_2 throughout the sampling period (Fig. 6). For S2, the only region that was not sampled during the night, the values of the diurnal differences obtained in S1 and S3 were applied, which seems reasonable, owing to their similar Chl *a* concentrations.

Comparing the three k_{600} used for the calculated fluxes, the k_{600} of Abril et al. (2009) can be considered the higher flux estimate, based on chamber measurements in 9 estuarine

systems, whereas the k_{600} of Wanninkhof (1992) provides a more conservative value. The model of Raymond and Cole (2001) based on non-intrusive "tracers only" data, provided intermediate fluxes compared to the other two models. k_{600} values varied from 0.8 to 12.3 cm h^{-1} , which correspond to wind speed velocities between 1.8 to 3.9 m s^{-1}. Current velocity (few dozen of centimeters per second) contributed to a minor fraction of k_{600} in the Abril et al. (2009) equation. On an annual basis, Guanabara Bay was a net sink of atmospheric CO_2 (year-integrated flux of -9.6, -12.0 and -18.1 mol C m^2 yr^{-1}, for k_{W02}, k_{RC01} and k_{A09}, respectively), but with strong differences at temporal and spatial scales. On a daily basis, summer CO_2 uptake was maximal in S3, S4 and S5, with daily fluxes of -190, -110 and -170 mmol C m^2 d^{-1}, respectively), whereas in the winter fluxes decreased to -14, -30 and +12 mmol C m^2 d^{-1}, respectively (note that S5 changed form a large sink in summer to a slight source in winter). S1 was a moderate source in winter (+60 mmol C m^2 d^{-1}) and a moderate sink in summer (-90 mmol C m^2 d^{-1}), as well as on an annual basis (-4.45 mol C m^2 yr^{-1}). In the highly polluted S2 sector, where a large part of the domestic organic matter is apparently respired, a strong annual outgassing occurred (+213 mmol C m^2 d^{-1}). However this region occupies only about 10% of the surface sampled area of the bay. It is interesting to note that at the midday/afternoon periods the winds were stronger than during the night/early-morning periods. This abides to the classical daily wind cycle at coastal regions guided by the thermal difference between the land and the water surface (Amarante et al., 2002), which apparently favors the CO_2 sink. Higher wind speed at daytime, and in summer also favored the CO_2 uptake.

The sink of CO_2 at air-sea interface showed values very close to the burial rates of organic carbon in the sediments. The table 3 presents one summary of the documented carbon fluxes in the Guanabara Bay. Carreira et al. (2002) found a 10-fold increase in the flux of organic carbon to the sediments in the last 50 years (maximum of 114 mmol C m^{-2} d^{-1} in the S5). Our annual budget of carbon uptake at the air-water interface was 105 mmol C m^2 d^{-1} for this same region, showing that Guanabara Bay is, in fact, a strong CO_2 sink and has an autotrophic metabolism. The autotrophic nature of Guanabara Bay is also confirmed by the relationship between autotrophic and heterotrophic communities (Guenther and Valentin, 2008; Guenther et al. 2008). Rebello et al. (1988) estimated phytoplankton primary production rates from monthly measurements over an annual cycle to vary between 60 to 300 mmol C m^{-2} d^{-1}, with highest rates in the lateral and upper

regions of the bay. The bacterial production used only a small fraction of the dissolved organic carbon pool, which had a turnover between 23 to 71 days in waters of the Bay (Guenther et al., 2008). Average net primary production (NPP) was 170 mmol C m^{-2} d^{-1}. Comparing with our results, the NPP values are very close to those found for the carbon uptake at air-water interface for summer conditions in the S3, S4 and S5, being 200, 149 and 189 mmol C m^{-2} $d^{-1,}$ respectively. After normalization to the total surface area of Guanabara Bay, the total average organic load from sewage and rivers is about 43 mmol OrgC m^2 d^{-1} (FEEMA, 1998), compared to the annual CO_2 uptake at the air-water interface of 49 mmol C m^2 d^{-1}. However, the pCO_2 spatial distribution supports the idea that most of the sewage-derived organic carbon is respired at the vicinity of the urban area, and little contributes to the carbon budget in the rest of the bay, except the Sector 2. In addition, molecular and isotopic characterization of the particulate organic matter of Guanabara Bay revealed the predominance of autochthonous organic matter (Kalas et al., 2009). Other fact that converges to the conclusion that Guanabara Bay behaves as a net autotrophic system is the high positive values of NCP in sectors 4 and 5. The annual average NCP was 143 mmol m^{-2} d^{-1}, and is the highest value compared to the compiled data set of Borges and Abril (2011) that included 79 estuaries, where 66 are net heterotrophic, 12 net autotrophic, and one balanced. The summertime period showed the highest values of NCP and coincides with the strongest sink of CO_2 at air-water interface. Guanabara Bay showed NCP values near that found in the tropical eutrophic Bojorquez Lagoon (Mexico) at the annual scale (Reyes and Merino, 1991) and in the subtropical coastal waters of Hong Kong at summertime (Yuan et al., 2011), both systems being highly impacted by sewage discharge.

5 Conclusions

In Guanabara Bay, annual uptake of atmospheric CO_2 associated with a net burial of organic matter in sediments was due to the synergic and cumulative effects of three factors: (i) an estuarine typology of marine dominated embayment with fairly long residence times of saline waters together with nutrient inputs in its upper sectors permitting phytoplanktonic developments; (ii) the tropical climatic conditions that increase light availability and favor the stratification of the water column; (iii) a long-term discharge of untreated domestic waters that have enriched the bay in nutrients and led to eutrophication. Eutrophication has also modified the phytoplanktonic assemblages

toward smaller, more productive and short-live groups (Villac and Tennenbaum, 2010), including some nitrogen-fixing species (cyanobacteria). A net autotrophic metabolism of Guanabara Bay is attested by the annual CO_2 uptake at the air-water interface, the positive and high NCP values, the low bacterial production relative to the primary production (Guenther et al., 2008), and the large burial of autochthonous organic carbon to the sediments (Carreira et al., 2002). It is the first estuarine system where the synergy of these three factors is clearly identified as the predominant driver of CO_2 dynamics and of carbon balance. Indeed, some other cases of net CO_2 uptake have been reported in some relatively polluted tropical coastal lagoons in Ivory Coast (Koné et al., 2010), in three temperate and marine-dominated Australian estuaries (Maher and Eyre, 2012), in temperate and tropical estuarine plumes either preserved (Körtzinger, 2003) or human-impacted (Cai, 2003; Zhai and Dai, 2009; Bozec et al., 2012), and in some pristine arctic and sub-artic fjords (Rysgaard et al., 2012; Ruiz-Halpern et al. 2010). In contrast, inner and low salinity regions of most river-dominated, drowned valley, "funnel-type" estuaries, which are generally well-mixed and relatively turbid environments, have been documented as heterotrophic and CO_2 emitters under tropical (Araujo et al., 2014), temperate (Frankignoulle et al. 1998) and boreal (Silveneoieen et al., 2008) climates and whatever the anthropogenic pressure (Abril et al., 2003; 2004; Zhai et al., 2007; Borges and Abril, 2011; Cai, 2011; Sarma et al., 2012).

Our findings of a net annual CO_2 sink in Guanabara Bay indicate that more field data are needed in particular in the highly productive tropical coastal ocean, in order to adequately integrate estuarine CO_2 fluxes at the global scale. In Brazil, most previous studies concerned river dominated estuaries, especially along the northern and northeastern coast, which all behave as CO_2 sources (Souza et al., 2009; Araujo et al., 2014; Noriega and Araujo, 2014). In contrast to Guanabara Bay, highest CO_2 fluxes correspond to denser population in the watersheds of these net heterotrophic systems (Noriega et al. 2014). In fact, the Brazilian coast presents several estuarine types (river estuarine deltas, estuaries, lagoons and large embayments) which have very different metabolisms (Bernardes et al., 2012), but where CO_2 fluxes have as yet to established. Large pCO_2 temporal variations can be expected for instance in a phytoplankton-dominated coastal lagoon in Brazil that exhibited an annually balanced metabolism, but with seasonal shifts between autotrophic and heterotrophic conditions (Carmouze et al., 1991; Knoppers et al. 1999a,b). Lagoons

dominated by macroalgae or microphytobenthos exhibited different metabolic trends, but still with a significant potential for a net uptake of atmospheric CO_2 (Knoppers, 1994). Undersampling coastal embayments and lagoons with clear and stratified waters, compared to turbid and well-mixed river-dominated estuaries, would potentially lead to an overestimation of the regional estuarine CO_2 budget. In addition, diurnal variations might impact the net CO_2 budget more significantly in autotrophic systems than in heterotrophic systems, and need to be assessed in the field. Continuous pCO_2 measurements on autonomous buoys (*e.g.* Frankignoulle et al., 2003; Bozec et al., 2011) are very promising tools to reach sufficient temporal resolution. We also showed that pCO2 dynamics were strongly correlated with meteorological conditions. Taking into account that the last projections of Intergovernmental Panel on Climate Change (IPCC) include unequivocal predictions of the climate system warming for the next years (Stocker et al., 2013), the increase of water temperature can reinforce the net sink of Guanabara Bay.

Acknowledgments

This research was funded by the Science without border program of the Brazilian National Council of Research and Development (CNPq-PVE 401726/2012-6). This project supported G.A. with a Senior Scientist grant, N.B. with a Post-Doc grant and LCCJr with a PhD grant for visiting EPOC. B.K. is a Senior Scientist of CNPq (Proc. Nr. 301572/2010-0). The meteorological data were kindly provided by the Brazilian Institute of Aerial Space Control (ICEA, Ministério da Defesa, Comando da Aeronáutica, Org. 2° SGT. BMT Antonio Carlos), and the global estuarine data by Dr Alberto Borges (Liège University). We are grateful to Wei-Jun Cai and the other anonymous referee for improving the quality of this manuscript with valuable suggestions and recommendations.

References

Abril, G., Nogueira, E., Hetcheber, H., Cabeçadas, G., Lemaire, E., and Brogueira, M.: Behaviour of organic carbon in nine contrasting European estuaries, Estuar. Coast. Shelf S., 54, 241–262, 2002.

Abril, G., Etcheber, H., Delille, B., Frankignoulle, M., and Borges, A.V.: Carbonate dissolution in the turbid and eutrophic Loire estuary, Mar. Ecol-Prog. Ser., 259, 129–138, 2003.

Abril G., Commarieu M., Maro D., Fontugne M., Guérin F., and Etcheber, H.: A massive dissolved inorganic carbon release at spring tide in a highly turbid estuary, Geophys. Res. Lett., 31, L09316, doi:10.1029/2004GL019714, 2004.

Abril, G., Richard, S., and Guérin, F.: In-situ measurements of dissolved gases (CH_4 and CO_2) in a wide range of concentrations in a tropical reservoir using an equilibrator, Sci. Total Environ, 354, 246–251, 2006.

Abril, G., Commarieu, M., Sottolichio, A., Bretel, P., and Guérin, F.: Turbidity limits gas exchange in a large macrotidal estuary, Estuar. Coast. Shelf Sci., 83, 342–348, 2009.

Allen, M. R., Frame, D. J., Huntingford, C., Jones, C., Lowe, J. A., Meinshausen, M., and Meinshausen, N.: Warming caused by cumulative carbon emissions towards the trillionth tonne, Nature, 458, 1163-1166, 2009.

Araujo, M., Noriega, C., and Lefèvre, N.: Nutrients and carbon fluxes in the estuaries of major rivers flowing into the tropical Atlantic, Frontiers in Marine Science, 1, 1–16, doi:10.3389/fmars.2014.00010, 2014.

Amarante, O. A., Silva, F. J., and Rios Filho, L. G.: Atlas Eólico, Estado do Rio de Janeiro, Secretaria de Estado da Energia, da Indústria Naval e do Petróleo, Rio de Janeiro, 64 pp., available at http://www.cresesb.cepel.br/publicacoes/download/atlas_eolico/AtlasEolicoRJ.pdf, 2002.

Bauer, J. E., Cai, W.J., Raymond, P., Bianchi, T. S., Hopkinson, C. S., and Regnier, P. G.: The changing carbon cycle of the coastal ocean, Nature, 504, 61–70, doi:10.1038/nature12857, 2013.

Benson, B.B. and Krause, D.: The concentration and isotopic fractionation of oxygen dissolved in freshwater and seawater in equilibrium with the atmosphere, Limnol. Oceanogr., 29, 620-632, 1984.

Bérgamo, A.S. 2010.: Caracteristicas hidrograficaz, da circulacao, e dos transportes de volume e sal na Baia de Guanabara (RJ) : variacoes sazonais e moduladas pela mare, Ph.D. thesis, Universidade de Sao Paulo, Sao Paulo, 200 pp., 2010.

Bernardes, M. C., Knoppers, B. A., Rezende, C. E., Souza, W. F., and Ovalle, A. R.: Land-sea interface features of four estuaries on the South America Atlantic coast, Braz. J. Biol., 72, 761-774, 2012.

Bidone, E. D. and Lacerda, L. D.: The use of DPSIR framework to evaluate sustainability in coastal areas. Case study: Guanabara Bay basin, Rio de Janeiro, Brazil, Reg. Environ. Change, 4, 5-16, 2004.

Borges, A. C., Sanders, C. J., Santos, H. L. R., Araripe, D. R., Machado, W., and Patchineelam, S. R.: Eutrophication history of Guanabara Bay (SE Brazil) recorded by phosphorus flux to sediments from a degraded mangrove area, Mar. Pollut. Bull., 58, 1750–1754, doi:10.1016/j.marpolbul.2009.07.025, 2009.

Borges, A. V. and Frankignoulle, M.: Daily and seasonal variations of the partial pressure of CO_2 in surface seawater along Belgian and southern Dutch coastal areas, J. Mar. Syst., 19, 251–266, doi:10.1016/S0924-7963(98)00093-1, 1999.

Borges, A. V.: Do we have enough pieces of the jigsaw to integrate CO_2 fluxes in the coastal ocean?, Estuaries, 28, 3–27, doi:10.1007/BF02732750, 2005.

Borges, A. V. and Gypens, N.: Carbonate chemistry in the coastal zone responds more strongly to eutrophication than ocean acidification, Limnol. Oceanogr., 55, 346–353, doi:10.4319/lo.2010.55.1.0346, 2010.

Borges, A.V. and G. Abril.: Carbon Dioxide and Methane Dynamics in Estuaries, in: Treatise on Estuarine and Coastal Science, Eric, W. and Donald, M. (eds.), Academic Press, Amsterdam, 119–161, 2011.

Bouillon, S., Borges, A. V., Castañeda-Moya, E., Diele, K., Dittmar, T., Duke, N. C, Kristensen, E., Lee, S. Y., Marchand, C., Middelburg, J. J., Rivera-Monroy, V., Smith T. J., and Twilley, R. R.: Mangrove production and carbon sinks: a revision of global budget estimates. Global Biogeochem. Cy., 22, GB2013, doi:10.1029/2007GB003052, 2008.

Bozec, Y., Merlivat, L., Baudoux, A. C., Beaumont, L., Blain, S., Bucciarelli, E., Danguy, T., Grossteffan, E., Guillot, A., Guillou, J., Répécaud, M., and Tréguer, P.: Diurnal to inter-annual dynamics of pCO_2 recorded by a CARIOCA sensor in a temperate coastal ecosystem (2003–2009), Mar. Chem., 126, 13–26, doi:10.1016/j.marchem.2011.03.003, 2011.

Bozec, Y., Cariou, T., Macé, E., Morin, P., Thuillier, D., and Vernet, M.: Seasonal dynamics of air-sea CO_2 fluxes in the inner and outer Loire estuary (NW Europe), Estuar. Coast. Shelf Sci., 100, 58–71, doi:10.1016/j.ecss.2011.05.015, 2012.

Bricker, S., Ferreira, J., and Simas, T.: An integrated methodology for assessment of estuarine trophic status, Ecol. Modell., 169, 39–60, doi:10.1016/S0304-3800(03)00199-6, 2003.

Bourton J. D. and Liss, P. S.: Estuarine Chemistry, Academic Press, London, 1976.

Cai, W. -J., Pomeroy, L. R., Moran, M. A., and Wang, Y. C.: Oxygen and carbon dioxide mass balance for the estuarine-intertidal marsh complex of five rivers in the southeastern US, Limnol. Oceanogr., 44, 639–649, 1999.

Cai, W.-J.: Riverine inorganic carbon flux and rate of biological uptake in the Mississippi River plume, Geophys. Res. Lett., 30, 1032, doi:10.1029/2002GL016312, 2003.

Cai, W.-J.: Estuarine and coastal ocean carbon paradox: CO_2 sinks or sites of terrestrial carbon incineration?, Annu. Rev. Mar. Sci., 3, 123–145, 2011.

Cai, W.-J., Hu, X., Huang, W.-J., Murrell, M. C., Lehrter, J. C., Lohrenz, S. E., Chou, W.-C., Zhai, W., Hollibaugh, J. T., and Wang, Y.: Acidification of subsurface coastal waters enhanced by eutrophication, Nat. Geosci., 4, 766–770, 2011.

Carmouze, J., Knoppers, B. A., and Vasconcelos, P. A.: Metabolism of Saquarema Lagoon, Brazil, Biogeochemistry, 2, 14, 129-148, 1991.

Carreira, R. S., Wagener, A. L. R., Readman, J. W., Fileman, T. W., Macko, S. A., and Veiga, Á.: Changes in the sedimentary organic carbon pool of a fertilized tropical estuary, Guanabara Bay, Brazil: an elemental, isotopic and molecular marker approach, Mar. Chem., 79, 207–227, doi:10.1016/S0304-4203(02)00065-8, 2002.

Chen, C. C., Gong, G. C., and Shiah, F. K.: Hypoxia in the East China Sea: One of the largest coastal low oxygen areas in the world, Mar. Environ. Res., 64, 399–408,

doi:10.1016/j.marenvres.2007.01.007, 2007.

Chen, C.T.A., Huang, T.H., Chen, Y.C., Bai, Y., He, X., and Kang, Y.: Air–sea exchanges of CO_2 in the world's coastal seas, Biogeosciences, 10, 6509–6544, doi:10.5194/bg-10-6509, 2013.

Chou, W. C., Gong, G. C., Cai, W. J., and Tseng, C. M.: Seasonality of CO_2 in coastal oceans altered by increasing anthropogenic nutrient delivery from large rivers: evidence from the Changjiang–East China Sea system, Biogeosciences, 10, 3889–3899, doi:10.5194/bg-103889-2013, 2013.

Cloern, J.: Our evolving conceptual model of the coastal eutrophication problem, Mar. Ecol. Prog. Ser., 210, 223–253, doi:10.3354/meps210223, 2001.

Cloern, J. E., Foster, S. Q., and Kleckner, A. E.: Phytoplankton primary production in the world's estuarine-coastal ecosystems, Biogeosciences, 11, 2477–2501, doi:10.5194/bg-11-2477-2014, 2014.

Cohen, J. E., Small, C., Mellinger, A., Gallup, J., and Jeffrey S.: Estimates of coastal populations, Science, 278, 1209-1213, 1997.

Dai, M., Zhai,W., Cai,W.-J., Callahan, J., Huang, B., Shang, S., Huang, T., Li, X., Lu, Z., Chen,W., Chen, Z.: Effects of an estuarine plume-associated bloom on the carbonate system in the lower reaches of the Pearl River estuary and the coastal zone of the northern South China Sea, Cont. Shelf Res, 28, 1416–1423, 2008.

Dai, M., Lu, Z., Zhai, W., Chen, B., Cao, Z., Zhou, K., Cai, W., and Chen, C. A.: Diurnal variations of surface seawater pCO_2 in contrasting coastal environments, Limnol. Oceanogr., 54, 735–745, 2009.

Dickson, A.G. and Millero, F.J.: A comparison of the equilibrium constants for the dissociation of carbonic acid in seawater media, Deep-Sea Res., 34, 1733–1743, 1987.

Doney, S. C., Fabry, V. J., Feely, R. A., and Kleypas, J. A.: Ocean Acidification: The Other CO 2 Problem, Annual Review of Marine Science, 1, 169–192, doi:10.1146/annurev.marine.010908.163834, 2009.

FEEMA:. Qualidade da agua da Baıa da Guanabara—1990 a 1997. Secretaria de Estado de Meio Ambiente, Fundaçao Estadual de Engenharia do Meio Ambiente, Rio de Janeiro, 187 pp., 1998.

Frankignoulle, M., Abril, G., Borges, A., Bourge, I., Canon, C., Delille, B., Libert, E., and Theate, J. M.: Carbon Dioxide Emission from European Estuaries, Science, 282, 434–436, 1998.

Frankignoulle, M., Borges A., and Biondo R.: A new design of equilibrator to monitor carbon dioxide in highly dynamic and turbid environments, Water Res., 35, 344 – 7, 2001.

Frankignoulle, M., Biondo, R., Théate, J. M., and Borges, A. V.: Carbon dioxide daily variations and atmospheric fluxes over the Great Bahama Bank using a novel autonomous measuring system. Caribb. J. Sci., 39, 257-264, 2003.

Gattuso J. P., Frankignoulle, M., and Wollast, R.: Carbon and carbonate metabolism in coastal aquatic ecosystems, Annu. Rev. Ecol. Syst., 29, 405-434, 1998.

Godoy, J. M., Moreira, I., Bragan, M. J., Wanderley, C., and Mendes, L. B.: A study of Guanabara Bay sedimentation rates, J. Radioanal. Nucl. Ch., 227, 157-160, 1998.

Grasshoff, K., Ehrhardt, M., and Kremling, K. (Eds.): Methods of Seawater Analysis, third ed., Wiley-VCH, Weinhein, 1999.

Guenther, M., Paranhos, R., Rezende, C., Gonzalez-Rodriguez, E., and Valentin, J.: Dynamics of bacterial carbon metabolism at the entrance of a tropical eutrophic bay influenced by tidal oscillation, Aquat. Microb. Ecol., 50, 123–133, doi:10.3354/ame01154, 2008.

Guenther, M. and Valentin, J.L. Bacterial and phytoplankton production in two coastal systems influenced by distinct eutrophication processes, Oecologia Brasiliensis, 12, 172-178, 2008.

Guenther, M., Lima, I., Mugrabe, G., Tenenbaum, D. R., Gonzalez-Rodriguez, E., and Valentin, J. L.: Small time scale plankton structure variations at the entrance of a tropical eutrophic bay (Guanabara Bay, Brazil), Braz. J. Oceanogr., 60, 405–414, 2012.

Guo, X., Cai, W.-J., Huang, W-J., Wang, Y., Chen, F., Murrell, M.C., Lohrenz, S. Dai, M., Jiang, L-Q. and Culp, R.: CO_2 dynamics and community metabolism in the Mississippi River plume. Limnol. Oceanogr., 57, 1-17, 2012.

Gypens, N., Borges, A. V., and Lancelot, C.: Effect of eutrophication on air-sea CO_2 fluxes in the coastal Southern North Sea: a model study of the past 50 years, Glob. Chang. Biol., 15, 1040–1056, doi:10.1111/j.1365-2486.2008.01773.x, 2009.

Huang, W-J., Cai, W-J., Wang, Y., Lohrenz, S.E., and Murrell, M.C.: The carbon dioxide (CO2) system on the Mississippi River–dominated continental shelf in the northern Gulf of Mexico – I: Distribution and air-sea CO2 flux, J. Geophy. Res., 120, 1429-1445, doi: 10.1002/2014JC010498, 2015.

Hunt, C. W., Salisbury, J. E., and Vandemark, D.: CO_2 Input Dynamics and Air–Sea Exchange in a Large New England Estuary, Estuar. Coast., 37, 1078–1091, doi:10.1007/s12237-013-9749-2, 2014.

Jiang, L. Q., Cai, W. J., and Wang, Y. C.: A comparative study of carbon dioxide degassing in river- and marinedominated estuaries, Limnol. Oceanogr., 53, 2603–2615, doi:10.4319/lo.2008.53.6.2603, 2008.

Jähne, B., Munnich, K. O., Bosinger, R., Dutzi, A., Huber, W., and Libner, P. On parameters influencing air-water exchange, J. Geophys. Res., 92, 1937–1949, 1987.

Kalas, F. A., Carreira, R. S., Macko, S. A., and R. Wagener, A. L.: Molecular and isotopic characterization of the particulate organic matter from an eutrophic coastal bay in SE Brazil, Cont. Shelf Res., 29, 2293–2302, doi:10.1016/j.csr.2009.09.007, 2009.

Kirk, J. T. O.: Light and Photosynthesis in Aquatic Ecosystems, 3rd edition, Cambridge University Press, New York, 2011.

Kjerfve, B., Ribeiro, C. A., Dias, G. T. M., Filippo, A., and Quaresma, V. S.: Oceanographic characteristics of an impacted coastal bay: Baia de Guanabara, Rio de Janeiro, Brazil, Cont. Shelf Res., 17, 1609–1643, 1997.

Knoppers, B.: Aquatic primary production in coastal lagoons, in: Coastal lagoon processes, Kjerfve, B., (Ed), Elsevier Science Publishers, Amsterdam, 243-286, 1994.

Knoppers, B. A., Carmouze, J. P., and Moreira-Turcqo, P. F.: Nutrient dynamics, metabolism and eutrophication of lagoons along the east Fluminense coast, state of Rio de Janeiro, Brazil, in: Environmental geochemistry of coastal lagoon systems of Rio de Janeiro, Brazil, Knoppers, B. A., Bidone, E. D., and Abrão, J. J., (Eds.), FINEP, Rio de Janeiro, 123-154, 1999a.

Knoppers, B., Ekau, W., and Figueiredo, A. G.: The coast and shelf of east and northeast Brazil and material transport, Geo-Mar. Lett., 19, 171-178, 1999b.

Koné, Y. J. M., Abril, G., Kouadio, K. N., Delille, B., and Borges, A. V.: Seasonal variability of carbon dioxide in the rivers and lagoons of Ivory Coast (West Africa), Estuar. Coast., 32, 246– 260, doi:10.1007/s12237-008-9121-0, 2009.

Körtzinger, A.: A significant CO_2 sink in the tropical Atlantic Ocean associated with the Amazon River plume, Geophys. Res. Lett., 30, 2287, doi:10.1029/2003GL018841, 2003.

Lee, K., Kim, T.W., Byrne, R. H., Millero, F. J., Feely, R. A., and Liu, Y.M.: The universal ratio of boron to chlorinity for the North Pacific and North Atlantic oceans, Geochim. Cosmochim. Ac., 74, 1801–1811, doi:10.1016/j.gca.2009.12.027, 2010.

Maher, D. T. and Eyre, B. D.: Carbon budgets for three autotrophic Australian estuaries: Implications for global estimates of the coastal air-water CO_2 flux, Global Biogeochem. Cy., 26, GB1032, doi:10.1029/2011GB004075, 2012.

Maher, D. T., Cowley, K., Santos, I., Macklin, P., and Eyre, B.: Methane and carbon dioxide dynamics in a subtropical estuary over a diel cycle: Insights from automated in situ radioactive and stable isotope measurements, Mar. Chem., 168, 69-79, 2015.

Matthews, H. D., Gillett, N. P., Stott, P. A., and, Zickfeld, K.: The proportionality of global warming to cumulative carbon emissions, Nature, 459, 829-832, 2009.

Mehrbach, C., Cuberson, C. H., Hawley, J.E., and Pytkowicz, R. M.: Measurements of the apparent dissociation constants of carbonic acid in seawater at atmospheric pressure. Limnol. Oceanog., 18, 897-907, 1973.

Monteiro, F., Cordeiro, R. C., Santelli, R. E., Machado, W., Evangelista, H., Villar, L. S., Viana, L. C. A., and Bidone, E. D.: Sedimentary geochemical record of historical anthropogenic activities affecting Guanabara Bay (Brazil) environmental quality, Environ. Earth Sci., doi: 10.1007/s12665-011-1143-4, 2011.

Monteith, J. L.: Climate and the efficiency of crop production in Britain, Philos. Trans. R. Soc. Lond. Ser. B, 281, 277–294, 1977.

Nixon, S. W.: Coastal marine eutrophication: a definition, social causes, and future concerns, Ophelia, 41, 199–219, 1995.

Noriega, C. and Araujo, M.: Carbon dioxide emissions from estuaries of northern and northeastern Brazil., Scientific Reports, 4, 6164, doi:10.1038/srep06164, 2014.

Noriega, C., Araujo, M., Lefèvre, N., Montes, M. F., Gaspar, F., and Veleda, D.: Spatial and temporal variability of CO_2 fluxes in tropical estuarine systems near areas of high population density in Brazil, Reg. Environ. Chang., 15, doi:10.1007/s10113-014-0671-3, 2014.

Orr, J. C., Fabry, V. J., Aumont, O., Bopp, L., Doney, S. C., Feely, R. a, Gnanadesikan, A., Gruber, N., Ishida, A., Joos, F., Key, R. M., Lindsay, K., Maier-Reimer, E., Matear, R., Monfray, P., Mouchet, A., Najjar, R. G., Plattner, G.-K., Rodgers, K. B., Sabine, C. L., Sarmiento, J. L., Schlitzer, R., Slater, R. D., Totterdell, I. J., Weirig, M.-F., Yamanaka, Y. and Yool, A.: Anthropogenic ocean acidification over the twenty-first century and its impact on calcifying organisms., Nature, 437, 681–6, 2005.

Paranhos, R., Pereira, A. P., and Mayr, L. M.: Diel variability of water quality in a tropical polluted bay, Environ. Monit. Assess., 50, 131–141, 1998.

Pritchard, D.W.: Estuarine Hydrography, Adv. Geophys., 1, 243-280, 1952.

Rabalais, N. N., Turner, R. E., Dıaz, R. J., and Justic, D.: Global change and eutrophication of coastal waters, ICES J. Mar. Sci., 66, 1528–1537, 2009.

Raymond, P.A. and Cole, J.J.: Gas exchange in rivers and estuaries: choosing a gas transfer velocity, Estuaries, 24, 312–317, 2001.

Rebello, A. L., Ponciano, C. R., and Melges, L. H.: Avaliacao da produtividade primaria e da disponibilidade de nutrientes na Baia de Guanabara, An. Acad. Bras. Cienc., 60, 419– 430, 1988.

Ribeiro, C. H. A. and Kjerfve, B.: Anthropogenic influence on the water quality in Guanabara Bay, Rio de Janeiro, Brazil, Reg. Env. Chan., 3, 13-19, 2001.

Robbins, L. L., Hansen, M. E., Kleypas, J. A., and Meylan. S. C.: CO2 Calc: a user-friendly seawater carbon calculator for Windows, Max OS X, and iOS (iPhone), U.S. Geological Survey Open-File Report, 2010–1280, 1–17, Available at: http://pubs.usgs.gov/of/2010/1280/, last access : 6 January 2013, 2010.

Ruiz-Halpern, S., Sejr, M. K., Duarte, C. M., Krause-Jensen, D., Dalsgaard, T., Dachs, J., and Rysgaard, S.: Air-water exchange and vertical profiles of organic carbon in a subarctic fjord, Limnol. Oceanogr., 55, 1733–1740, doi:10.4319/lo.2010.55.4.1733, 2010.

Rysgaard, S., Mortensen, J., Juul-Pedersen, T., Sorensen, L. L., Lennert, K., Sogaard, D. H., Arendt, K. E., Blicher, M. E., Sejr, M. K., and Bendtsen, J.: High air-sea CO_2 uptake rates in nearshore and shelf areas of Southern Greenland: Temporal and spatial variability, Mar. Chem., 128, 26–33, doi:10.1016/j.marchem.2011.11.002, 2012.

Sabine, C. L., Feely, R. a, Gruber, N., Key, R. M., Lee, K., Bullister, J. L., Wanninkhof, R., Wong, C. S., Wallace, D. W. R., Tilbrook, B., Millero, F. J., Peng, T.-H., Kozyr, A., Ono, T., and Rios, A. F.: The oceanic sink for anthropogenic CO_2, Science, 305, 367–71, doi:10.1126/science.1097403, 2004.

Santos, V. S., Villac, M. C., Tenenbaum, D. R., and Paranhos, R.: Auto-and heterotrophic nanoplankton and filamentous bactéria of Guanabara Bay (RJ, Brazil): estimates of cell/ filament numbers versus carbon content, Braz. J. Oceanogr., 55, 133-143, 2007.

Sarma, V., Viswanadham, R., Rao, G. D., Prasad, V. R., Kumar, B. S. K., Naidu, S. A., Kumar, N. A., Rao, D. B., Sridevi, T., Krishna, M. S., Reddy, N. P. C., Sadhuram, Y., and Murty, T. V. R.: Carbon dioxide emissions from Indian monsoonal estuaries, Geophys. Res. Lett., 39, L03602, doi:10.1029/2011gl050709, 2012.

Silvennoinen, H., Liikanen, A., Rintala, J., and Martikainen, P. J.: Greenhouse gas fluxes from the eutrophic Temmesjoki River and its Estuary in the Liminganlahti Bay (the Baltic Sea), Biogeochemistry, 90, 193–208, doi:10.1007/s10533-008-9244-1, 2008.

Smith, S.V.; Swaney, D.P., Talaue-McManus, L. Carbon–Nitrogen–Phosphorus fluxes in the coastal zone: The LOICZ approach to global assessment, in: Carbon and nutrient fluxes in continental margins, Liu, K., Atkinson, L., Quiñones, R., Talaue-McManus, L., (Eds.), Springer-Verlag Berlin Heidelberg, Berlin, 575-586, 2010.

Souza, M., Gomes, V., Freitas, S., Andrade, R., and Knoppers, B.: Net ecosystem metabolism and nonconservative fluxes of organic matter in a tropical mangrove estuary, Piauí River (NE of Brazil), Estuar. Coast., 32, 111–122, doi:10.1007/s12237-008- 9104-1, 2009.

Stocker, T. F., Qin, D., Plattner, G. K., Tignor, M., Allen, S. K., Boschung, J., Nauels, A., Xia, Y., Bex, V., and Midgley, P. M. (Eds.): Climate Change 2013: The Physical Science Basis. Contribution of Working Group I to the Fifth Assessment Report of the Intergovernmental Panel on Climate Change, Cambridge University Press, United Kingdom, 2013.

Strickland J. D. H. and Parsons T.R.: A practical handbook of seawater analysis, second ed., Fisheries Research Board of Canada Bulletin, Ottawa, Canada, 1972.

Sunda, W. G. and Cai, W.J.: Eutrophication Induced CO_2-Acidification of Subsurface Coastal Waters: Interactive Effects of Temperature, Salinity, and Atmospheric pCO_2. Environ. Sci. Technol., 46, 10651–10659, doi: 10.1021/es300626f, 2012.

Takahashi, T., Sutherland, S.C., Sweeney, C., Poisson, A., Metzl, N., Tilbrook, B., Bates, N., Wanninkhof, R., Feely, R.A., Sabine, C., Olafsson, J. and Nojiri, Y.: Global sea–air CO_2 flux based on climatological surface ocean pCO_2, and seasonal biological and temperature effects, Deep-Sea Res. Part II, 49, 1601–1622, 2002.

Valentin, J. L., Tenenbaum, D. R., Bonecker , A. C. T., Bonecker, S. L. C., Nogueira, C. R., and Villac, M. C.: O sistema planctônico da Baía de Gaunabara: Síntese do conheciemnto. In: Silva, S.H.G.; Lavrado, H.P. (Eds). Ecologia dos Ambientes Costeiros do estado do Rio de Janeiro, Oecologia Brasiliensis, 7, 35-59, 1999.

Villac, M. C. and Tenenbaum, D. R.: The phytoplankton of Guanabara Bay, Brazil. I. Historical account of its biodiversity, Biota Neotropic, 10, 271-293, 2010.

Wallace, R. B., Baumann, H., Grear, J. S., Aller, R. C., and Gobler, C. J.: Coastal ocean acidification: The other eutrophication problem, Estuar. Coast Shelf S., 148, 1-13, 2014.

Wollast, R.: Evaluation and comparison of the global carbon cycle in the coastal zone and in the open ocean, in: The Sea, Vol. 10, Brink, K. H. and Robinson, A. R. (Eds.), John Wiley & Sons, New York, 213–252, 1998.

Weiss, R. F.: Carbon dioxide in water and seawater: the solubility of a non-ideal gas, Mar. Chem., 2, 203–215, 1974.

Yates, K. K., Dufore, C., Smiley, N., Jackson, C., and Halley, R. B.: Diurnal variation of oxygen and carbonate system parameters in Tampa Bay and Florida Bay, Mar. Chem., 104, 110–124, doi:10.1016/j.marchem.2006.12.008, 2007.

Zhai, W., Dai, M., and Guo, X.: Carbonate system and CO_2 degassing fluxes in the inner estuary of Changjiang (Yangtze) River, China, Mar. Chem., 107, 342–356, doi:10.1016/j.marchem.2007.02.011, 2007.

Zhai, W. D. and Dai, M. H.: On the seasonal variation of air-sea CO_2 fluxes in the outer Changjiang (Yangtze River) Estuary, East China Sea, Mar. Chem., 117, 2–10, doi:10.1016/j.marchem.2009.02.008, 2009.

Zhang, L., Xue, M. and Liu, Q.: Distribution and seasonal variation in the partial pressure of CO_2 during autumn and winter in Jiaozhou Bay, a region of high urbanization., Mar. Pollut. Bull., 64, 56–65, doi:10.1016/j.marpolbul.2011.10.023, 2012.

Zhang, C., Huang, H., Ye, C., Huang, L., Li, X., Lian, J. and Liu, S.: Diurnal and seasonal variations of carbonate system parameters on Luhuitou fringing reef, Sanya Bay, Hainan Island, South China Sea, Deep Sea Res. Part II Top. Stud. Oceanogr., 96, 65–74, doi:10.1016/j.dsr2.2013.02.013, 2013

Table 1. Mean **(±** standard deviation), minimum, maximum and number of observations (N) of the principal physicochemical properties of the waters of Guanabara Bay for the sampling period separated by sectors.

	Sector 1	Sector 2	Sector 3	Sector 4	Sector 5
Temp. (°C)	23.8 ± 1.7 (21.0 - 29.3) N = 1918	25.5 ± 2.2 (22.1 - 32.4) N = 1047	25.4 ± 2.1 (22.1 - 31.5) N = 2035	26.8 ± 2.6 (22.0 - 32.3) N = 1594	26.7 ± 2.2 (22.6 - 33.9) N = 2397
Salinity	32.2 ± 2.1 (25.4 - 34.9) N = 1918	30.3 ± 2.4 (17.7 - 33.7) N = 1047	29.8 ± 3.0 (15.1 - 33.8) N = 2035	27.0 ± 4.3 (14.6 - 33.2) N = 1594	27.2 ± 3.5 (16.6 - 32.9) N = 2397
DO (%)	103 ± 29 (48 - 221) N = 1918	97 ± 59 (2 - 263) N = 1047	138 ± 51 (56 - 357) N = 2035	142 ± 62 (30 - 361) N = 1594	160 ± 69 (46 - 370) N = 2397
pCO_2 (ppmv)	411 ± 145 (104 - 747) N = 1918	711 ± 561 (50 - 3715) N = 1046	286 ± 157 (41 - 660) N = 2035	307 ± 256 (29 - 2222) N = 1594	272 ± 293 (22 - 2203) N = 2397
pH (NBS)	8.20 ± 0.16 (7.90 - 8.71) N = 1581	8.15 ± 0.32 (7.33 - 8.96) N = 910	8.35 ± 0.23 (7.88 - 8.96) N = 1790	8.34 ± 0.29 (7.39 - 9.01) N = 1490	8.44 ± 0.31 (7.51 - 9.23) N = 2225
TA ($\mu mol.kg^{-1}$)	2240 ± 92 (1942 - 2320) N = 44	2291 ± 99 (1890 - 2488) N = 32	2168 ± 177 (1507 - 2500) N = 40	2045 ± 369 (2111 - 3920) N = 39	2137 ± 166 (1479 - 2314) N = 53
DIC ($\mu mol.kg^{-1}$)	1985 ± 120 (1720 - 2127) N = 44	2044 ± 268 (1526 - 2523) N = 32	1847 ± 257 (1332 - 2290) N = 32	1658 ± 259 (1095 - 2118) N = 35	1758 ± 264 (1198 - 2190) N = 52
Chl-*a* ($\mu g.L^{-1}$)	19.1 ± 22.0 (2.0 - 128.0) N= 34	46.2 ± 51.4 (3.3 - 212.9) N= 33	57.6 ± 90.0 (1.6 - 537.2) N= 33	69.2 ± 60.2 (13.1 - 288.8) N= 32	107.7 ± 101.8 (1.5 - 822.1) N= 47
NO_3-N (µM)	3.50 ± 3.30 (0.13 - 12.50) N= 34	3.72 ± 4.93 (< LD - 18.63) N= 33	4.12 ± 5.27 (0.16 - 19.12) N= 32	2.14 ± 3.29 (< LD - 14.74) N= 33	1.92 ± 2.08 (0.04 - 9.20) N= 47
NO_2-N (µM)	1.60 ± 1.92 (0.05 - 7.30) N= 36	2.59 ± 2.89 (0.10 - 10.67) N= 33	1.81± 2.58 (< LD - 10.79) N= 33	1.46 ± 2.74 (0.03 - 9.37) N= 33	1.71 ± 1.98 (0.03 - 7.08) N= 47
NH_4-N (µM)	8.15 ± 6.26 (0.09 - 22.50) N=37	44.9 ± 25.2 (0.15 - 94.73) N= 33	9.10 ± 9.48 (0.04 - 37.95) N= 33	4.96 ± 6.92 (0.04 - 29.29) N= 33	26.82 ± 27.67 (0.13 - 130.12) N= 47
PO_4-P (µM)	1.11 ± 0.60 (0.11- 2.44) N= 37	5.28 ± 3.88 (0.17 - 20.79) N= 33	1.51 ± 1.07 (0.17 - 1.10) N= 33	1.10 ± 0.79 (0.03 - 2.96) N= 33	2.23 ± 2.17 (0.02 - 8.72) N= 47

Table 2 Summary of calculated mean values for wind speed (U_{10}), gas exchange coefficient (k_{600}) and CO_2 fluxes at the air-sea interface in each sectors and entire Guanabara Bay. Diurnal variations (nighttime < 9:30 AM; daytime > 9:30 PM) seasonal means (winter and summer) and time-integrated values are reported. W92 are the data calculated according to k_{600} of Wanninkhof (1992), RC01 are the data calculated according to k_{600} of Raymond and Cole (2001), and A09 are data calculated according to k_{600} of Abril et al. (2009).

			U_{10} ($m\ s^{-1}$)	k_{600} ($cm\ h^{-1}$)			CO_2 Flux ($mmol\ m^{-2}\ h^{-1}$)		
				W92	RC01	A09	W92	RC01	A09
Sector 1	Winter	Nightime	1.8	1.2	3.5	7.2	0.55	1.59	3.37
($47Km^2$)		Daytime	2.5	2.6	4.7	9.0	0.50	1.19	2.33
	Summer	Nightime	2.5	2.7	4.8	9.2	-0.84	-1.27	-2.35
		Daytime	3.8	6.6	8.5	12.3	-1.23	-3.88	-5.42
	Time-integrated		2.6	3.2	5.3	9.4	-0.25	-0.57	-0.51
Sector 2	Winter	Nightime	1.9	1.9	3.7	7.5	5.19	7.74	14.61
($32Km^2$)		Daytime	2.4	2.3	4.4	8.8	3.29	4.99	10.29
	Summer	Nightime	2.5	3.1	4.8	9.2	1.75	1.97	2.87
		Daytime	3.3	4.4	6.2	10.9	1.12	1.28	2.02
	Time-integrated		2.5	2.9	4.7	9.1	2.27	4.00	7.44
Sector 3	Winter	Nightime	1.4	0.8	3.0	6.1	-0.13	0.06	0.34
($96Km^2$)		Daytime	2.6	2.8	4.9	9.2	-0.19	-0.79	-1.53
	Summer	Nightime	2.8	3.0	5.0	9.7	-1.97	-3.28	-6.37
		Daytime	3.9	6.7	8.4	12.2	-4.82	-6.22	-9.65
	Time-integrated		2.6	3.3	5.3	9.3	-1.77	-2.56	-4.29
Sector 4	Winter	Nightime	1.5	0.9	3.2	6.2	-0.10	-0.33	-0.59
($55Km^2$)		Daytime	2.3	2.3	4.4	7.8	-1.04	-1.26	-2.00
	Summer	Nightime	2.1	1.7	4.0	7.4	-0.24	-0.43	-0.76
		Daytime	3.2	4.6	6.4	9.9	-4.28	-5.90	-9.13
	Time-integrated		2.2	2.3	4.5	7.8	-1.41	-1.97	-3.12
Sector 5	Winter	Nightime	1.5	0.9	3.2	6.1	0.83	3.32	5.88
($80Km^2$)		Daytime	2.4	2.4	4.5	8.0	-1.61	-2.67	-4.87
	Summer	Nightime	2.1	1.8	4.0	7.4	-2.67	-3.25	-4.99
		Daytime	3.1	4.2	6.0	9.6	-4.27	-6.21	-9.73
	Time-integrated		2.2	2.3	4.4	7.7	-1.93	-2.20	-3.42
All Bay	Winter	Nightime					0.78	1.86	3.53
($310Km^2$)		Daytime					-0.24	-0.46	-0.67
	Summer	Nightime					-1.29	-1.92	-3.45
		Daytime					-3.42	-5.02	-7.73
	Time-integrated						-1.10	-1.38	-2.07

Table 3 Summary of the documented carbon fluxes in the Guanabara Bay.

Inputs	*mmol C m^{-2} d^{-1}*	*Comment*
CO_2 air-water flux	26 – 49*	All bay average; This study
CO_2 air-water flux	33 – 102*	Sectors 3, 4 and 5; This study
Organic carbon load from sewage	43	All bay average; FEEMA (1998), majority of organic carbon seems to be mineralized in sewage network
River DIC, DOC and TOC inputs	Undocumented	
Internal Processes	*mmol C m^{-2} d^{-1}*	*Comment*
NCP	51 – 225 (143)**	Sectors 4 and 5; This study
NPP	60 – 300 (170)**	Sectors 2, 3 and 5; Rebello et al., (1988)
Total Respiration	Undocumented	
Outputs	*mmol C m^{-2} d^{-1}*	*Comment*
Organic carbon burial	27 – 114	Sectors 3, 4 and 5; Carreira et al., (2002); Monteiro et al., (2011)
DIC and TOC export to the coastal area	Undocumented	

*Annual average according to the k600 model parameterizations of Wanninkhof (1992) and Abril et al., (2009). The lower value refers to the model of Wanninkhof (1992), whereas the higher value refers to the model of Abril et al. (2009).

** Range and annual average in parenthesis.

Figure Captions

Figure 1. Map of Guanabara Bay. Dark grey color indicates the urbanized areas. Green color shows the mangrove localization. Black points represent the locations of the discrete sampling, black lines are isobaths, red squares represent the locations of the airports with the meteorological stations, and blue lines delimit the different sectors in the bay (sectors S1 to S5).

Figure 2. Meteorological conditions during the sampling period (in green) compared with historical values (1951-2014, in blue). 2a presents the monthly accumulated precipitation; 2b presents the monthly average of atmospheric temperature.

Figure 3. Typical vertical profiles of salinity, temperature, dissolved oxygen (DO) and chrollophyll *a* (Chl *a*) in the water column. Profiles are showed for S1, S3 and S5, in summer and winter conditions. Note the different depth scale for the S5. Dotted line in 3k and 3l shows nighttime profile (7:00 AM), whereas full line shows a daytime profile (12:30 PM) the same day at the same station.

Figure 4. Concentration maps of continuous pCO_2 measurements in surface waters of Guanabara Bay for all the sampling campaigns.

Figure 5. Diurnal variations of pCO_2 concentrations. The ship back and forth tracks are indicated as red lines in small maps. Arrows show the boat direction and sampling time are indicated along each track. Blue parts of the tracks are considered as nighttime (< 9:30 AM) and green parts as daytime (> 9:30 AM). Inserted small graphs also show the water pCO_2 evolution *versus* time, and shadow area represents the sampling before 9:30 AM (nighttime). The grey lines indicate the atmospheric pCO_2 (400 ppmv). Note the different pCO_2 scales for each survey.

Figure 6. Box plots (maximum, percentile 75%, median, percentile 25% and minimum) of pCO_2 data for all the campaigns (a), and for each individual sectors (b, c, d, e and f). Black box plots represents the nighttime data (< 9:30 AM), when available, and white box plots represent daytime data (> 9:30 AM).

Figure 7. Relationship between the excess dissolved inorganic carbon (E-DIC) and apparent utilization of oxygen (AOU) in Guanabara Bay (green dots) compared to those reported in 24 estuarine environments (red dots, Borges and Abril, 2011). The 1:1 line represents the quotient between CO_2 and O_2 during the processes of photosynthesis and respiration.

Figure 8. Principal Components Analysis (PCA) based on mean values for each sampling campaign of the physical and biogeochemical properties of the water (temperature, salinity, pCO_2, DO and Chl *a*) and meteorological conditions (wind velocity and accumulated precipitation of 7 days before each survey). The data-set was normalized by z-scores.

Figure 1

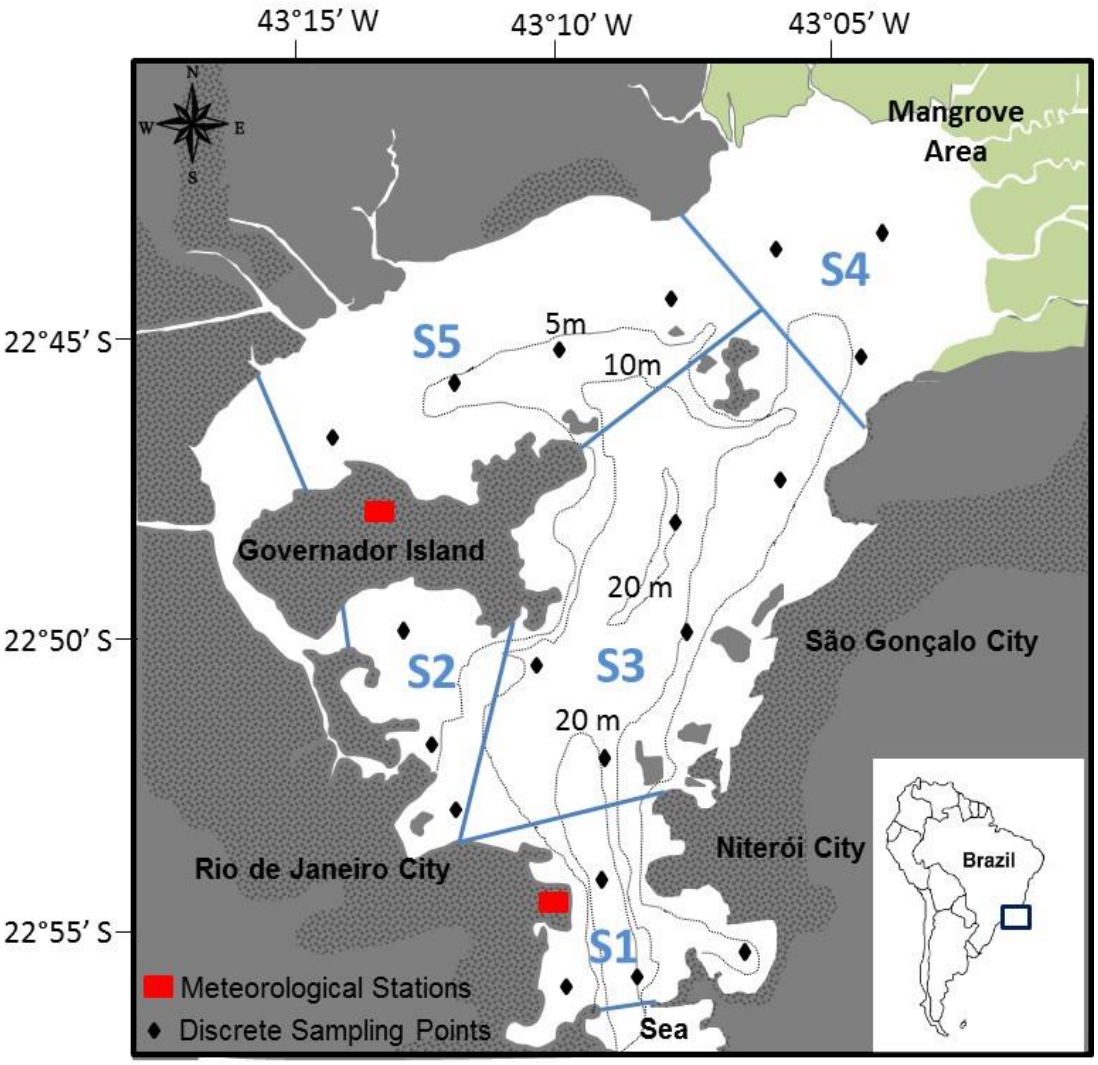
43°15' W
43°10' W
43°05' W
22°45' S
22°50' S
22°55' S
N
W
E
S
Mangrove Area
S4
S5
5m
10m
Governador Island
20 m
São Gonçalo City
S2
S3
20 m
Niterói City
Rio de Janeiro City
S1
Meteorological Stations
Discrete Sampling Points
Sea
Brazil

Figure 2

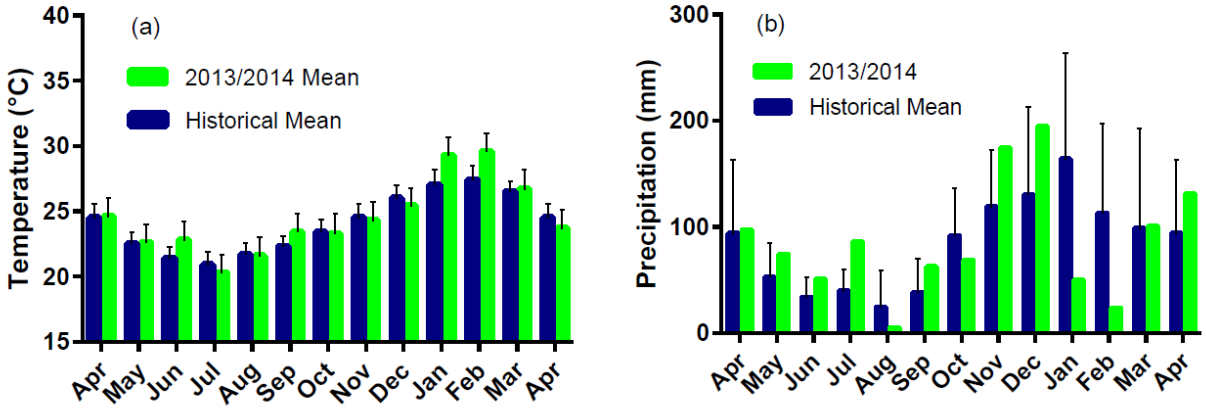
(a)
2013/2014 Mean
Historical Mean
Temperature (°C)
40
35
30
25
20
15
Apr
May
Jun
Jul
Aug
Sep
Oct
Nov
Dec
Jan
Feb
Mar
Apr
(b)
2013/2014
Historical Mean
Precipitation (mm)
300
200
100
0
Apr
May
Jun
Jul
Aug
Sep
Oct
Nov
Dec
Jan
Feb
Mar
Apr

Figure 3

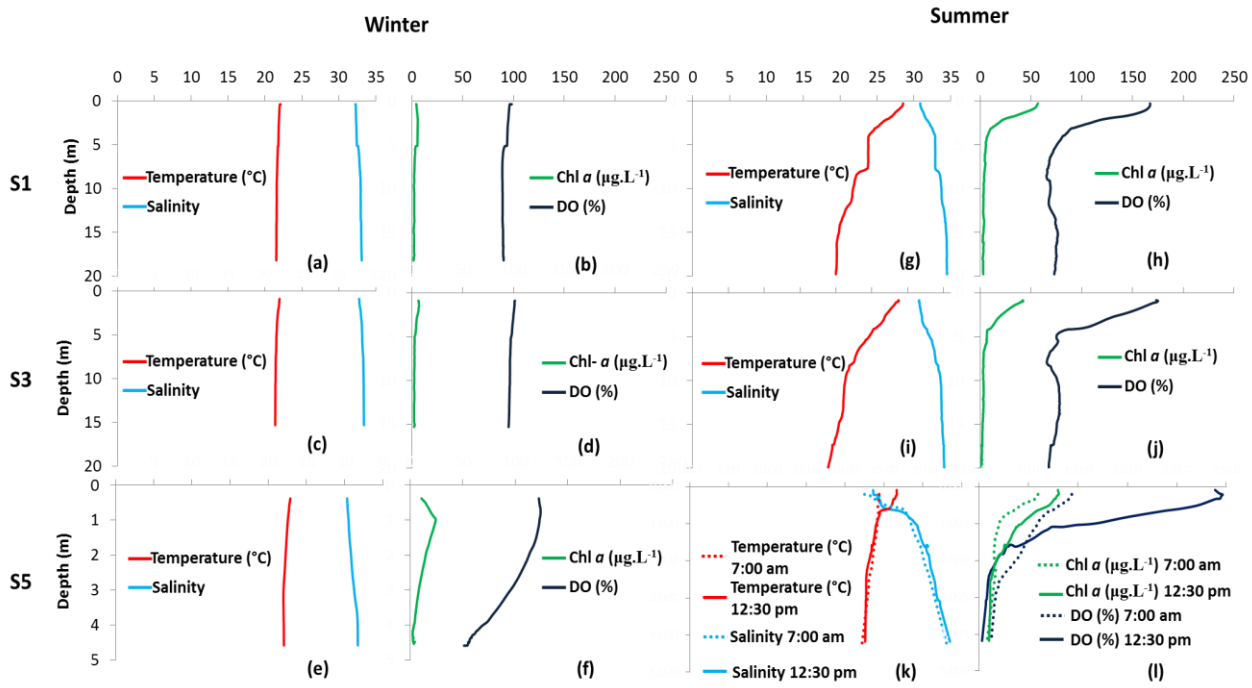
Winter
Summer
S1
S3
S5
Depth (m)
Temperature (°C)
Salinity
Chl a (µg.L-1)
Chl- a (µg.L-1)
DO (%)
Temperature (°C) 7:00 am
Temperature (°C) 12:30 pm
Salinity 7:00 am
Salinity 12:30 pm
Chl a (µg.L-1) 7:00 am
Chl a (µg.L-1) 12:30 pm
DO (%) 7:00 am
DO (%) 12:30 pm
(a)
(b)
(c)
(d)
(e)
(f)
(g)
(h)
(i)
(j)
(k)
(l)

Figure 4

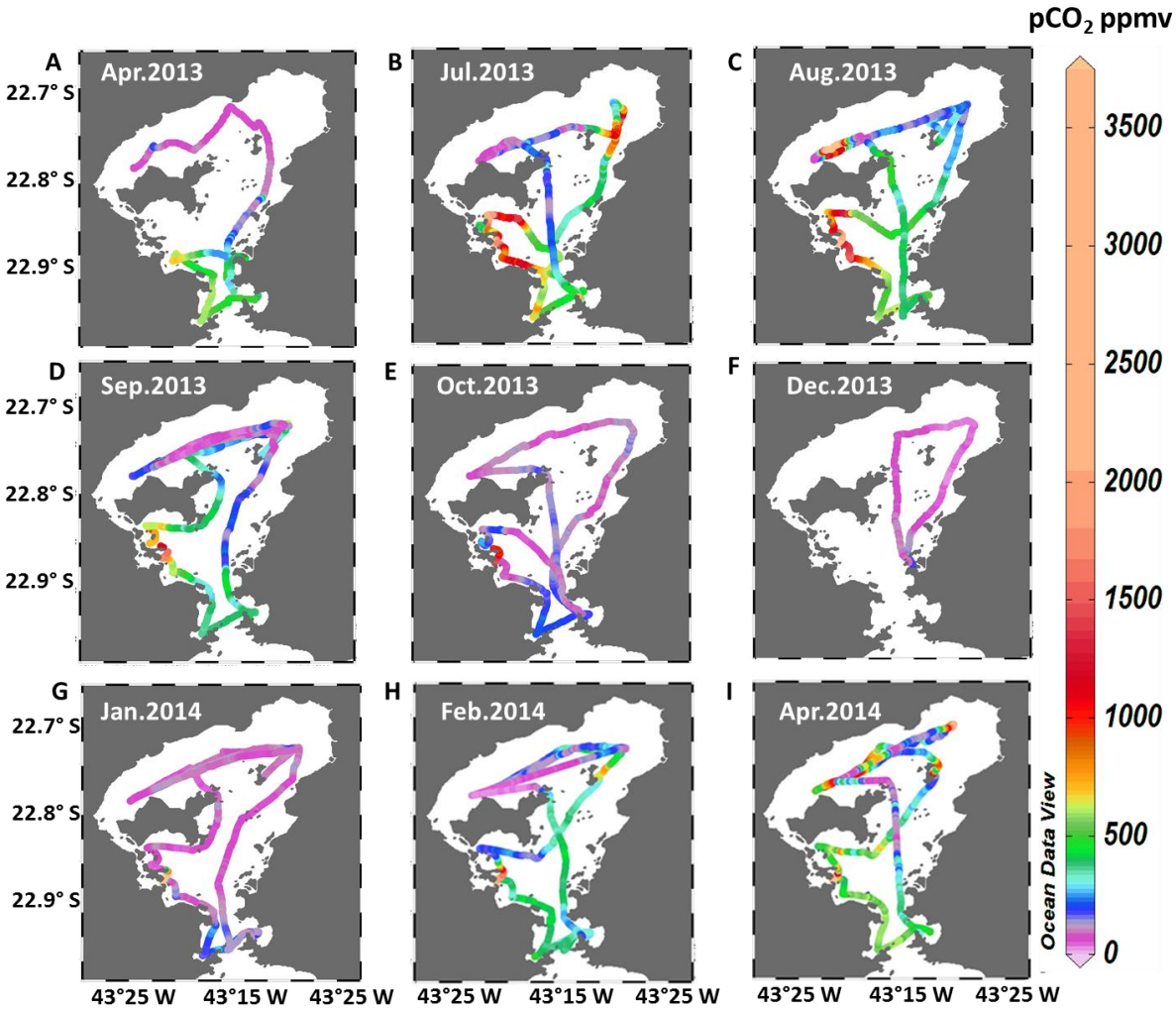
pCO2 ppmv
A
Apr.2013
B
Jul.2013
C
Aug.2013
D
Sep.2013
E
Oct.2013
F
Dec.2013
G
Jan.2014
H
Feb.2014
I
Apr.2014
22.7° S
22.8° S
22.9° S
43°25 W
43°15 W
43°25 W
3500
3000
2500
2000
1500
1000
500
0
Ocean Data View

Figure 5

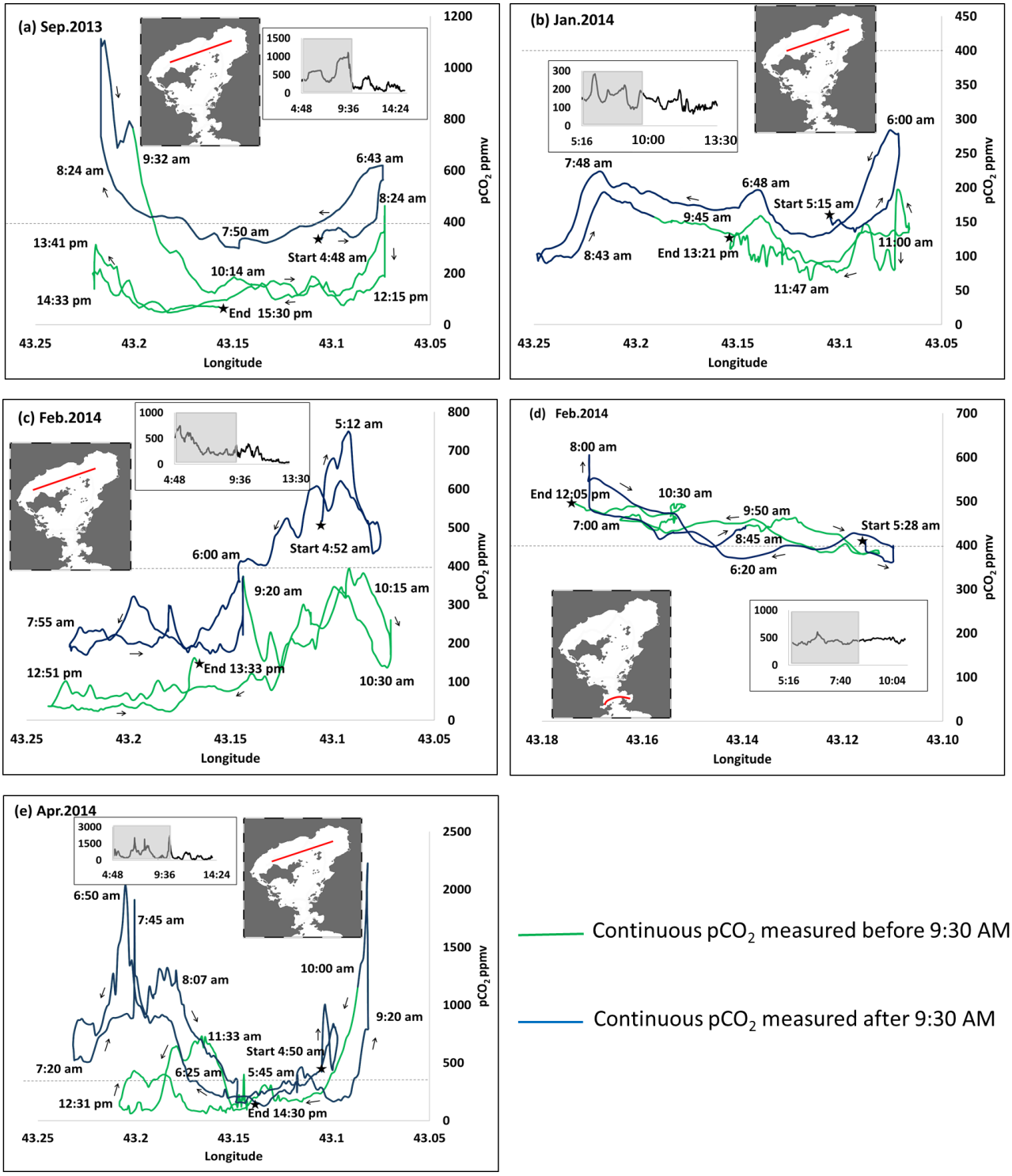
(a) Sep.2013
9:32 am
8:24 am
6:43 am
8:24 am
7:50 am
13:41 pm
Start 4:48 am
10:14 am
14:33 pm
12:15 pm
End 15:30 pm
Longitude
(b) Jan.2014
6:00 am
7:48 am
6:48 am
Start 5:15 am
9:45 am
11:00 am
8:43 am
End 13:21 pm
11:47 am
Longitude
(c) Feb.2014
5:12 am
Start 4:52 am
6:00 am
9:20 am
10:15 am
7:55 am
12:51 pm
End 13:33 pm
10:30 am
Longitude
(d) Feb.2014
8:00 am
End 12:05 pm
10:30 am
9:50 am
7:00 am
Start 5:28 am
8:45 am
6:20 am
Longitude
(e) Apr.2014
6:50 am
7:45 am
10:00 am
8:07 am
9:20 am
11:33 am
Start 4:50 am
7:20 am
6:25 am
5:45 am
12:31 pm
End 14:30 pm
Longitude
pCO2 ppmv
Continuous pCO2 measured before 9:30 AM
Continuous pCO2 measured after 9:30 AM

Figure 6

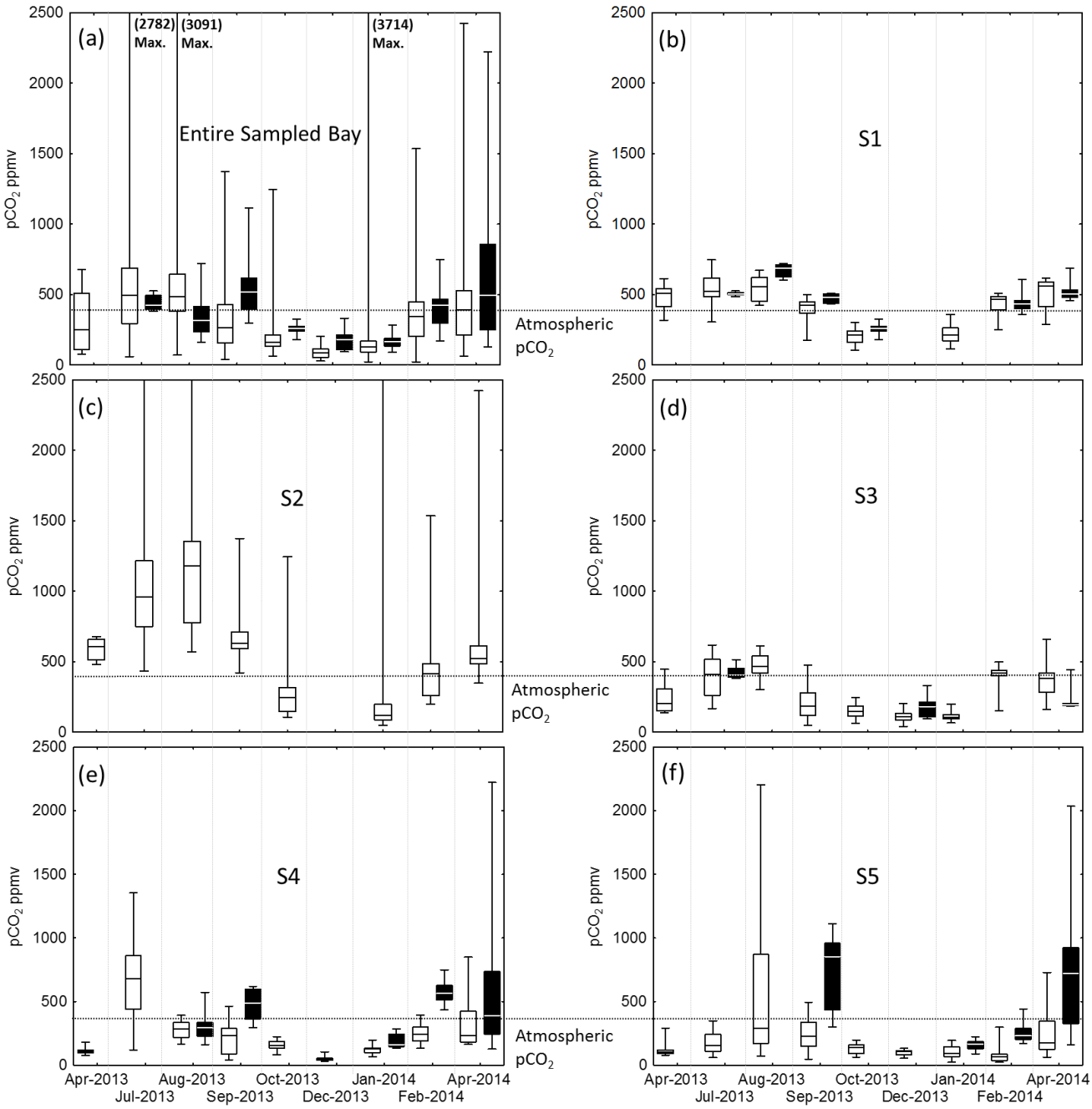
(a)
(2782) Max.
(3091) Max.
(3714) Max.
Entire Sampled Bay
(b)
S1
(c)
S2
(d)
S3
(e)
S4
(f)
S5
pCO2 ppmv
Atmospheric pCO2
0
500
1000
1500
2000
2500
Apr-2013
Jul-2013
Aug-2013
Sep-2013
Oct-2013
Dec-2013
Jan-2014
Feb-2014
Apr-2014

Figure 7

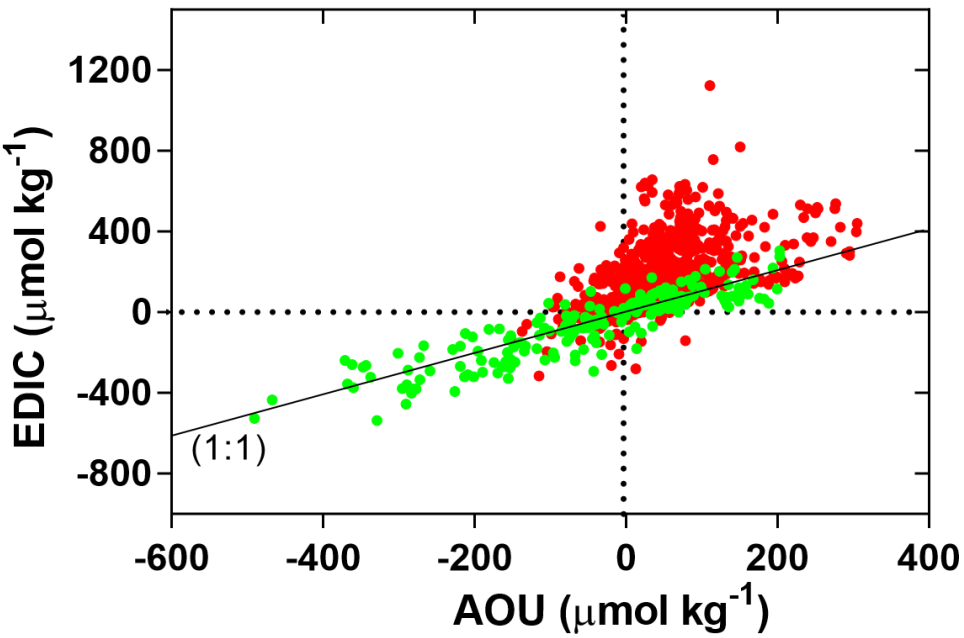
1200
800
400
0
-400
-800
EDIC (μmol kg-1)
(1:1)
-600
-400
-200
0
200
400
AOU (μmol kg-1)

Figure 8

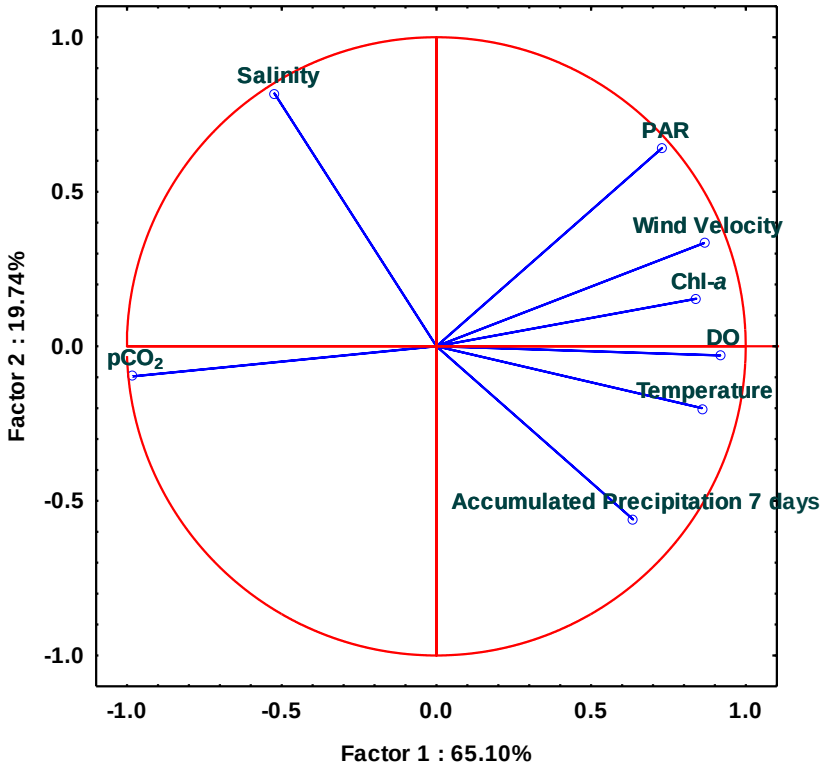
1.0
0.5
0.0
-0.5
-1.0
Factor 2 : 19.74%
-1.0
-0.5
0.0
0.5
1.0
Factor 1 : 65.10%
Salinity
PAR
Wind Velocity
Chl-a
DO
pCO2
Temperature
Accumulated Precipitation 7 days